Nano-Fe2O3 as a tool to restore plant growth in contaminated soils – Assessment of potentially toxic elements (bio)availability and redox homeostasis in Hordeum vulgare L

Andrés Rodríguez-Seijo, Cristiano Soares, Sónia Ribeiro, Berta Ferreiro Amil, Carla Patinha, Anabela Cachada, Fernanda Fidalgo, Ruth Pereira

Nano-Fe_2O_3 as a tool to restore plant growth in contaminated soils - Assessment of potentially toxic elements (bio)availability and redox homeostasis in *Hordeum vulgare* L.

Cite this article as:

Rodríguez-Seijo A, Soares C, Ribeiro S, Amil BF, Patinha C, Cachada A, Fidalgo F, Pereira R. 2022. Nano-Fe_2O_3 as a tool to restore plant growth in contaminated soils - Assessment of potentially toxic elements (bio)availability and redox homeostasis in *Hordeum vulgare* L. Journal of Hazardous Materials 425, 127999. http://doi.org/10.1016/j.jhazmat.2021.127999

The final publication is available at ELSEVIER http://doi.org/10.1016/j.jhazmat.2021.127999

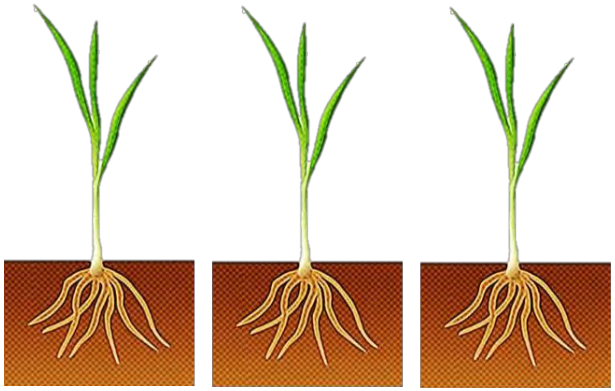

OECD soil
(control)

S1 **S2**
Contaminated agricultural soils

Can **nano-Fe_2O_3** protect plant growth in **contaminated soils**?

PTEs immobilization & bioaccumulation

Addition of **nano-Fe_2O_3** to S1 and S2 **Mixed effects on elements' availability**

However:

The **nano-Fe_2O_3** amendment **did not majorly change** the **accumulation pattern of PTEs**

Plant growth and redox status

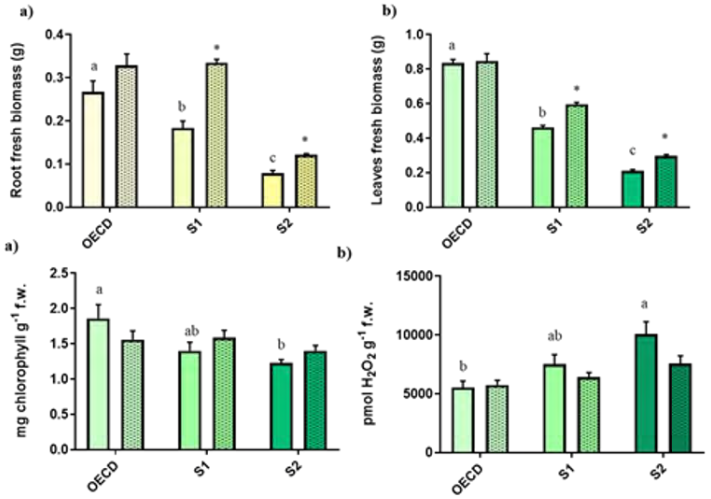

Bars with pattern → + nano-Fe_2O_3

S1 and S2

- Reduced growth performance;
- Decrease of total chlorophylls and increase of H_2O_2 levels.

OXIDATIVE STRESS
(especially in S2)

+ nano-Fe_2O_3

Alleviation of the negative effects, with a better growth capacity of both leaves and roots.

Highlights:

- The two contaminated soils greatly impaired plant growth.

- Nano-Fe_2O_3 can protect the growth of barley plants under contaminated soils.

- A better physiological performance accompanied the positive effects on growth.

- The application of nano-Fe_2O_3 helped to limit the oxidative damage.

-Plants increased their antioxidant response when grown in soils treated with nano-Fe_2O_3.

Nano-Fe_2O_3 as a tool to restore plant growth in contaminated soils - assessment of potentially toxic elements (bio)availability and redox homeostasis in *Hordeum vulgare* L.

Andrés Rodríguez-Seijo[1,2*], Cristiano Soares[2,3*], Sónia Ribeiro[2,3], Berta Ferreiro Amil[3,4], Carla Patinha[5], Anabela Cachada[1,2], Fernanda Fidalgo[2,3], Ruth Pereira[2,3]

[1]CIIMAR - Interdisciplinary Centre of Marine and Environmental Research (CIIMAR), University of Porto, Terminal de Cruzeiros do Porto de Leixões, Av. General Norton de Matos s/n, 4450-208, Matosinhos, Portugal

[2]Department of Biology, Faculty of Sciences of University of Porto (FCUP), 4169-007 Porto, Portugal

[3]GreenUPorto—Sustainable Agrifood Production Research Centre and INOV4AGRO, Rua do Campo Alegre s/n, Faculty of Sciences of University of Porto (FCUP), 4169-007 Porto, Portugal

[4]Faculdade de Bioloxía, Universidade de Santiago de Compostela, Santiago de Compostela, Spain

[5]Department of Geosciences & GEOBIOTEC, University of Aveiro, Campus de Santiago, Aveiro, 3810-193, Portugal

* These authors contributed equally to this work and, therefore, should be both considered as first co-authors

‡*Corresponding author:*

Andrés Rodríguez-Seijo (andres.seijo@fc.up.pt)

Abstract: This work aimed to evaluate the potential of Fe_2O_3 nanoparticles (nano-Fe_2O_3) to alleviate potentially toxic elements (PTEs) - induced stress in barley plants *(Hordeum vulgare* L.), focusing on bioaccumulation patterns and on plant growth and redox homeostasis. To achieve this goal, plants grew in two agricultural soils, contaminated by different levels of PTEs, collected from an industrial area, previously amended, or not, with 1% (w/w) nano-Fe_2O_3. After 14 d of growth, biometric parameters were evaluated, along with the analysis of PTEs bioaccumulation and biochemical endpoints. After exposure to contaminated soils, plant development was greatly affected, as evidenced by significant decreases in root length and biomass production. However, upon co-treatment with nano-Fe_2O_3, lower inhibitory effects on biometric parameters were observed. Regarding the oxidative damage, both soils led to increases in lipid peroxidation and superoxide anion concentration, though hydrogen peroxide levels were only increased in the most contaminated soil. In general, these changes in the oxidative stress markers were accompanied by an upregulation of different antioxidant mechanisms, whose efficiency was even more powerful upon soil amendment with nano-Fe_2O_3, thus lowering PTEs-induced oxidative damage. Altogether, the present study revealed that nano-Fe_2O_3 can protect the growth of barley plants under contaminated soils.

Keywords: abiotic stress; soil contamination; bioaccumulation; nanomaterials, soil functions

1. Introduction

Industrial and commercial activities are the second source of soil contamination in the European Union (EU), with adverse effects on nearby aquatic and terrestrial ecosystems, and subsequent impacts on human health (Panagos et al. 2013). Due to the lack of environmental guidelines or mismanagement practices, industrial wastes and gas emissions were released to the surrounding environments during decades without any environmental management (Wuana and Okieimen 2011; Panagos et al. 2013).

Multiple techniques have been developed to reduce soil contamination, such as phytoremediation, excavation, and transport to landfill sites, soil washing or electrokinetic remediation (Komárek et al. 2013). However, chemical immobilization has been pointed out as a very suitable technique for soil rehabilitation, due to its practical and cost-effective features, being regarded as a more environmentally friendly practice for reducing contaminants' availability through co-precipitation, complexation. or sorption mechanisms (Komárek et al. 2013; Arenas-Lago et al. 2016, 2019; Rizwan et al. 2019).

For several years, organic amendments have been widely used for these purposes, but nanotechnology applications, such as the use of nanomaterials (NMs), are becoming increasingly popular due to their low cost and higher effectiveness for potentially toxic elements (PTEs) immobilization in multi-contaminated soils and to improve plant growth in these phytotoxic soils, thus recovering soil production function (Komárek et al. 2013; Gil-Díaz et al. 2016, Rizwan et al. 2019; Soares et al. 2018a; Song et al. 2019).

Among all metal-based NMs, Fe-NMs (nano-Fe_xO_y) are one of the most applied, being able to interact directly with other PTEs, such as As, Cd, Cr, Cu, Pb or Zn. Moreover, as reviewed by Tripathi et al. (2017), nano-Fe_xO_y are narrowly absorbed by plants and barely translocated to aerial parts, preventing the over-accumulation of Fe along food chains, as well as Fe-induced toxicity in plants. Up to now, studies have focused on the advantages of Fe-NMs as nanofertilizers (Ruttkay-Nedecky et al. 2017; Hussain et al. 2019; Rizwan et al. 2019), but information about their impact on plant abiotic stress responses, namely on reducing PTEs uptake and bioaccumulation, along with their interference on the redox metabolism, is still limited (Ruttkay-Nedecky et al. 2017; Song et al. 2019). Regarding this aspect, it has recently been shown that Zn oxide (nano-ZnO) and Fe oxide (nano-Fe_3O_4) could be used to improve plant growth under Cd-induced toxicity (Hussain et al. 2018; Rizwan et al. 2019), by reducing metal bioaccumulation and by improving the overall physiological status of plants.

In response to plant exposure to any type of abiotic stress, including exposure to PTEs, plants usually undergo a state of oxidative stress, in which overproduction of reactive oxygen species (ROS) and subsequent damage in biomolecules take place (Soares et al. 2019a). In order to counteract the toxic effects of ROS, plants have evolved a powerful and complex antioxidant system, whose action depends on both enzymatic (e.g. superoxide dismutase – SOD, EC1.15.1.1; catalase – CAT, EC 1.11.1.6; ascorbate peroxidase – APX, EC 1.11.1.11) and non-enzymatic (e.g., ascorbate – AsA; glutathione – GSH; proline – Pro) players (Soares et al. 2019a). In this sense, pinpointing the regulation of redox homeostasis of plants under stress can provide important clues regarding the responses to PTEs exposure, as well as concerning the potential of NM-based amendments to reduce PTEs-induced stress. However, such studies are still in the beginning, since they have mostly been performed under controlled conditions with spiked artificial soils, or by simulating single contamination scenarios (Komárek et al. 2013; Ruttkay-Nedecky et al. 2017; Song et al. 2019).

In this way, this study aims to go one step forward by evaluating the ability of hematite NMs (nano-Fe_2O_3) to immobilize PTEs present in natural contaminated soils, while also contributing for a better crop performance in areas affected by industrial activities. To achieve this, the bioavailability of PTEs was studied using two chemical extractions methods ($CaCl_2$ and EDTA), and through bioaccumulation assays with barley plants (*Hordeum vulgare* L.). To understand if the application of nano-Fe_2O_3 is also able to decrease PTEs-exposure and subsequent induced stress, biometric parameters, along with the physiological performance and redox homeostasis of barley plants, were evaluated. Since oxidative stress occurrence is a common feature of PTEs phytotoxicity, special attention was paid to the oxidative metabolism, by the quantification of oxidative stress markers (lipid peroxidation and ROS levels) and by the evaluation of the non-enzymatic and enzymatic antioxidant system components.

2. Materials and Methods

2.1. Sampling area, soil samples and characterization of studied soils.

The Estarreja Chemical Complex (ECC), located in northwestern Portugal (Figure S1 in Supplementary Material), includes one of the largest companies in the Iberian Peninsula that produces aniline and chlor-alkali products. During decades and up to the 90s of the last century, these industries released wastewater directly into a nearby lagoon (Lagoon of Aveiro) through a system of channels and pipes that cross agricultural fields and contained several inorganic and organic contaminants (Costa and Jesus-Rydin 2001; Pereira et al. 2009; Inácio et al. 2014). As a result, a large amount of solid wastes, rich in PTEs, was

94 stockpiled during decades without any impermeabilization measures (Costa and Jesus-Rydin 2001), and
95 high levels of PTEs in soils located near the ECC have been reported, especially close to the wastewater
96 channels used to transport effluents (e.g., Batista et al. 2002; Cachada et al. 2009; Inácio et al. 2014).
97 For the present study, two agricultural soils (S1 and S2) were collected near a channel that was formerly
98 used to transport untreated effluents from the EEC (Figure S1). Once in the laboratory, samples were air-
99 dried, passed through a 2 mm (for physical-chemical properties) or a 4 mm sieve (for plant assays), and
100 homogenized before the experimental analyses. Soil pH and electrical conductivity were measured in 1:5
101 (w/v) soil-deionized water suspension. The maximum soil water holding capacity (WHC_{max}) was
102 determined according to ISO 11268-2 (ISO, 2012). The organic matter was measured according to, the loss-
103 on-ignition method (450 °C, 8 h) (British Standards 2000), while soil texture was analyzed using the pipette
104 method (Gee and Bauder, 1986). The pseudo total content of As, Ba, Cd, Cr, Cu, Fe, Mg, Ni, Pb, Sb, Zn
105 and P was measured after using a mixture of nitric acid and hydrochloric acid 3:1 (v/v) for a wet digestion
106 of soil samples in a microwave (Ethos 1; Milestone), following the method 3051A from USEPA (USEPA,
107 2007). The determination of PTEs and P content in the extracts was carried out by Inductively Coupled
108 Plasma Optical Emission Spectroscopy (ICP-OES) (PE 4300 DV). The accuracy and the precision of the
109 analytical method included replicates, procedure blanks, and NIST SRM 2711a as certified reference
110 material. Replicate analysis of the soil gave an uncertainty <10%. The results of blank analysis were always
111 below the detection limit, and reference material recoveries were within the certified value.

112 *2.2. Soil amendment with hematite NM and assessment of the immobilization effectiveness*

113 The hematite NM (nano-Fe_2O_3) was purchased from IOLITEC (Ionic liquids Technologies GmbH,
114 Germany). The selected NM is a powder, with semi-spherical form particles, dark brown color, 98% purity,
115 a diameter between 20 and 40 nm, and a surface area between 40–60 $m^2 g^{-1}$, corroborating the
116 manufacturer's characteristics. The shape, size, surface area and chemical composition were verified by
117 HR-TEM/EDS analysis (CACTI, UVigo, Spain). More details about their characterization can be found in
118 Arenas-Lago et al. (2019).
119 To assess the immobilization efficiency of this NM, the studied soils (S1 and S2) were spiked with a
120 suspension of the NM to obtain a dose of 1% (w/w) in the soil, since this is the optimal concentration for
121 stabilization of PTEs from soil, according to Komárek et al. (2013) and Martínez-Fernández et al. (2015).
122 The experiments for the soil amended with hematite were performed by following the methodology

123 indicated by Arenas-Lago et al. (2016, 2019) and Rodríguez-Seijo et al. (2020). Briefly, a suspension of
124 the hematite NM was prepared in distilled water (5 g L^{-1}). Sodium citrate (5 mM) was added as a stabilizer,
125 and the final pH obtained was 7.10 ± 0.15. After that, 10 g of each studied soil were treated with 20 mL of
126 the NM suspension in polypropylene tubes. Control samples (non-amended soils) were also prepared, using
127 the same amount of soil and distilled water. Three replicates were prepared for both treatments (non- and
128 amended with nano-Fe_2O_3). After shaking the soil suspensions during 24 h at 120 rpm in an orbital platform
129 shaker, they were kept in darkness, at room temperature, for 10 d of stabilization. Then, samples were dried
130 at 30 °C and homogenized to assess the chemical available content of PTEs.

131 *2.2.1. Available contents of PTEs for non- and amended soil samples.*

132 The effect of soil amendment on the chemical availability of PTEs was evaluated for non- and amended
133 soil samples using calcium chloride ($CaCl_2$) [0.01 M, 2 h of shaking, 1:10 (w/v) (Houba et al. (2000)] and
134 ethylenediaminetetraacetic acid (EDTA) [0.05 M at pH 7, 1 h of shaking, 1:10 (w/v) (Quevauviller (1998)].
135 After shaking, the soil suspensions were centrifuged (1937 *g* for 30 min), the supernatants were separated
136 and acidified, followed by the determination of PTEs concentration by ICP-MS. The extraction efficiency
137 (EE) was calculated for each extractant in each soil before and after treatment with nano-Fe_2O_3 (Equation
138 1):

139 $$\text{Extraction efficiency (EE)} = [100 \times (Ce/Ct)] \quad \text{(Equation 1)}$$

140 where *Ce* and *Ct* are the concentration of the element extracted (with $CaCl_2$ or EDTA) and the pseudo total
141 content of each PTEs (mg kg^{-1}), respectively.

142 *2.3. Test-species, plant growth conditions and experimental design*

143 To test the effectiveness of nano-Fe_2O_3 to reduce the bioavailability of PTEs, and consequently their
144 bioaccumulation and phytotoxicity, a seedling emergence and growth test with barley plants (*Hordeum*
145 *vulgare* L.) was performed, following the OECD 208 (2006) guidelines. Before the beginning of the assay,
146 seeds purchased from a local supplier were surface sterilized [10 min in 70% (v/v) ethanol; 7 min in 20%
147 (v/v) sodium hypochlorite (5% (v/v) active chlorine) containing 0.05% (w/v) Tween-20] and washed with
148 multiple cleanups using deionized water. Then, plastic pots (0.3 L) were filled with 200 g dry weight (dw)
149 of each studied soil (S1 and S2), previously amended, or not, with 1% of nano-Fe_2O_3 (as detailed in section
150 2.2.). In parallel, an artificial soil (herein named as OECD soil) with 5% (w/w) organic matter and pH 6.0
151 ± 0.5 (OECD, 2006) was used as control. All soil samples (S1, S2 and OECD) were manually mixed to

obtain a homogeneous mixture (Gil-Díaz et al. 2016; Arenas-Lago et al. 2019) and eight pots were considered for each experimental group (48 pots in total). The pots were filled with each soil and wetted with the nanomaterial suspension until the soil had a value of 50% of the water holding capacity and were kept in the dark at 20 ± 2 °C for 48 h to allow an initial stabilization of the mixtures (Gil-Diaz et al. 2016; García-Gómez et al. 2018). After this period, 20 barley seeds were placed in each pot. At the beginning of the assay, a commercial fertilizer (NPK 6-3-7), diluted according to supplier instructions, was added to a cup placed below each pot, being the communication between both ensured by a cotton rope to allow the nutrients solution and then the water to ascend by capillarity. After seed germination, only 7 plantlets were left to grow for additional 14d to avoid intraspecific competition. The experiment was performed in a growth chamber under controlled conditions (temperature: 22 ± 1 °C; photoperiod: 16 h light/8 h dark; light intensity: 120 μmol m^{-2} s^{-1}). During the growth period, the water level was adjusted whenever needed with deionized water, to guarantee the necessary conditions of soil moisture. At the end of the experiment, four replicates of each treatment, randomly selected, were used for the evaluation of biometric parameters and PTEs bioaccumulation. In the other four replicates, the leaves were separated from roots, washed with deionized water, and immediately frozen under liquid nitrogen and stored at -80 °C until posterior use for biochemical assays. For all biochemical assays (2.5.1-2.5.4), frozen leaf samples from at least 3 experimental replicates were analyzed independently.

2.4. Biometric parameters and bioaccumulation of PTEs in barley

After the growth period, plants were thoroughly washed several times, firstly with tap water, and secondly with distilled water, to remove as much as possible soil particles adhered to their surface. After that, the biomass (fresh mass) of leaves and roots was recorded for each replicate. The root length was also recorded for each plantlet in each replicate.

Afterwards, roots and leaves from each plant from four experimental replicates were dried in an oven at 60 °C until reaching constant mass. Finally, after weighting the dry biomass, leaves were grounded and used for the analysis of PTEs. For each replicate, around 0.2 g of sample were digested with H_2O_2 and HNO_3 [1:3 (v/v)] in a heating block (DigiPREP MS, SCP Science). The digests were diluted to 50 mL with Milli-Q water, and the PTEs content was determined by Inductively Coupled Plasma Mass Spectrometry (ICP-MS) (Agilent 7700). Each extraction batch included the analysis of blanks (always below detection limit) and a reference material (ERM-CD200), for which the recoveries were within the certified value.

Besides, the bioconcentration factor (BCF) was calculated for plants collected from S1 and S2 soils amended and non-amended with the hematite NM. These analyses were not conducted in the OCED soils. The BCF in plants was determined by calculating the ratio between the concentration of a given PTE in the plant (C*p*) to that in the soil (C*so*), as given below (Equation 2):

$$BCF = Cp / Cso \qquad (Eq.\ 2)$$

2.5. Biochemical parameters

2.5.1 *Quantification of photosynthetic pigments*

The extraction and quantification of photosynthetic pigments (total chlorophylls and carotenoids) was performed in frozen aliquots of leaves (ca. 200 mg) based on the protocol of Lichtenthaler (1987) and the results expressed as mg g^{-1} fresh mass (f.m.).

2.5.2. Assessment of oxidative stress markers: ROS levels and lipid peroxidation (LP)

The determination of reactive oxygen species (ROS) included the determination of superoxide anion ($O_2^{\cdot-}$) and hydrogen peroxide (H_2O_2) contents. For both analyses, samples of leaves (200 mg) were used. Levels of $O_2^{\cdot-}$ were spectrophotometrically quantified according to the methods of Gajewska and Skłodowska (2007). Results were expressed in terms of $Abs_{580\ nm}$ h^{-1} g^{-1}f.m. Regarding H_2O_2, its content was quantified by a colorimetric method as described by Jana and Choudhuri (1982) and the results were expressed as pmol H_2O_2 g^{-1}f.m. Lipid peroxidation (LP), evaluated by the quantification of malondialdehyde (MDA), was performed according to, the protocol of Heath and Packer (1968). MDA content of each sample was expressed as nmol g^{-1}f.m. More details on each protocol can be found in Soares et al. (2019b).

2.5.3. Quantification of non-enzymatic antioxidants: proline, glutathione and ascorbate

The levels of proline and glutathione were spectrophotometrically quantified based on the ninhydrin (Bates et al. 1973) and Ellman's reagent colorimetric assay, respectively, following the exact procedure detailed by Soares et al. (2019b). Concerning ascorbate, its total, reduced (AsA) and oxidized (dehydroascorbate – DHA) content were determined in leaves as described by Gillespie and Ainsworth (2007), using the 4,4'-bipyridyl (BIP) colorimetric method. Results were expressed in µg g^{-1}f.m. (Pro) and µmol g^{-1}f.m. (AsA and GSH).

2.5.4. Quantification of enzymatic antioxidants – SOD, APX and CAT activity

208 The extraction of the main antioxidant enzymes was performed as previously reported (Soares et al. 2019b).
209 After centrifugation, the supernatant of each sample was used for total protein quantification (Bradford
210 1976) and the determination of SOD, CAT and APX activity. In the case of SOD, NaN_3 was added to a
211 final concentration of 10 µM. The total activity of SOD, APX and CAT were evaluated according to, the
212 original protocols developed by Donahue et al. (1997), Nakano and Asada (1994) and Aebi (1984),
213 respectively. SOD was expressed in terms of units SOD mg^{-1} protein, being one SOD unit defined as the
214 amount of enzyme that inhibits by 50% the photochemical reduction of NBT. CAT was expressed in nmol
215 H_2O_2 min^{-1} mg^{-1} protein, while APX activity values were reported as µmol DHA min^{-1} mg^{-1} protein. A
216 detailed description of each assay can be found in Soares et al. (2019b).

217 *2.6. Statistical analyses*

218 Results from all biometric and biochemical parameters were expressed as the mean ± standard deviation
219 (SD). After verifying the homogeneity of the variances (Levene test), a bi-factorial analysis of variance
220 (two-way ANOVA) was performed, defining as fixed factors the soil and the hematite amendment, and
221 assuming a significance value of 0.05. In cases of significant differences for any of the factors, a one-way
222 ANOVA was performed to test for significant differences between amended soils; when the interaction
223 between factors was significant, the one-way ANOVA was performed with correction for the simple main
224 effects. All statistical procedures were performed in Prism 8 (GraphPad Software Inc, USA) and IBM SPSS
225 Statistics v23 (IBM®, USA).

226 **3. Results**

227 *3.1 Physicochemical properties of soils*

228 The properties of the studied soil samples are shown in Table 1. Results revealed a very strong acidic (S1)
229 to slightly acid (S2) pH, low (S1) to medium (S2) content of organic matter and low electrical conductivity
230 values (Zdruli et al. 2004; Costa 2011; Soil Science Division Staff 2017). The soil texture was sandy loam,
231 according to USDA classification, for both samples (Soil Science Division Staff 2017). The mean values
232 of the pseudo total concentration of PTEs are also shown in Table 1. Comparing with the guideline values
233 from Portugal and Canada, S2 showed high levels of As, Ba, Cu, Pb, and Zn, while S1 displayed low levels
234 of PTEs, all below the guidelines, except for As.

235 **[Table 1]**

236 *3.2. Available content of PTEs in soils: the effect of hematite NM amendment*

237 The available content of the studied PTEs in the soils was assessed by two single extractions ($CaCl_2$ and
238 EDTA). Additionally, the extraction efficiency (EF) was calculated for each extractant in each soil before
239 and after soils amendment with nano-Fe_2O_3 (Table 2). In the non-amended soils (S1 and S2) the $CaCl_2$-
240 extractable concentrations of PTEs were low (<7 % of the pseudo total content), except for Cd in S1. The
241 amendment of soils with nano-Fe_2O_3 significantly increased the $CaCl_2$-extracted concentrations of Mn (S1
242 and S2), Mg (S1), Ba (S2) and Sb (S2), but decreased the available Zn (S1). The EDTA-extractable PTEs
243 were higher than the $CaCl_2$-extractable levels, in both non-amended soils, but in particular for Cd, Cu, Pb
244 and Zn. The amendment of soils with the NM significantly decreased the EDTA extractable concentration
245 of Cd, Cu, K, Mg, Ni, Sb, Pb and Zn (in S2), but increased the availability of other elements, such as Mn
246 (S1 and S2) (Table 2).

247 **[Table 2]**

248 *3.3. Accumulation of PTEs by plants in non- and amended soils with nano-Fe_2O_3*

249 The amendment of soils with the NM did not majorly contribute to reduce the PTEs accumulation by leaves
250 of barley plants, except for Cd and Zn in plants from S1 and Sb in plants from S2. In parallel, plants grown
251 in the OCED soil amended with the NM presented a significant increment of Fe levels (Table 3). Regarding
252 BCF values, a significant reduction was also observed for Ni and Sb in S2, and Zn in S1. Besides, BCF
253 values of studied elements in leaves of barley were less than 1, except for Cd, Mn and Zn in S1, indicating
254 that these elements were not accumulated in the aerial parts of plants (Table 3).

255 **[Table 3]**

256 *3.4. Biometric parameters and biomass production*

257 Root length and fresh biomass of leaves and roots were affected by both factors (soil type and hematite
258 amendment), which showed a significant interaction between each other (Tables S3 and S4). As can be
259 observed in Figure 1, when plants were grown in S1 and S2, the root length was reduced by 55 and 75%,
260 respectively, in comparison with those grown in OECD artificial soil (control). This pattern was also
261 observed for biomass production, especially in S2, where root and leaf growth were inhibited up to 75% in
262 relation to the OECD soil. However, when soils were amended with nano-Fe_2O_3, a high average root length
263 (73% and 54% high in S1 and S2, respectively) was registered, in comparison with the non-amended soils.

Roots and leaves biomass were also stimulated by the application of the NM, with significant increases in comparison with their non-amended counterparts.

[Figure 1]

3.5. Photosynthetic pigments – total chlorophylls and carotenoids

According to the statistical analysis, only the type of soil (OECD, S1 and S2) significantly affected the levels of total chlorophylls (a + b) and carotenoids (Tables S3 and S4). When barley plants were exposed to S2, total chlorophylls were reduced by 34%, in relation to the OECD soil (Figure 2). Regarding S1, no statistical differences from the control soil were recorded (Figure 2).

[Figure 2]

3.6 Oxidative stress markers – ROS levels and LP

The modulation of $O_2^{\cdot-}$ levels by the soil amendment with nano-Fe_2O_3 was dependent on the soil (Tables S3 and S4). Although no changes were found between non-amended soils and the control, the application of nano-Fe_2O_3 displayed a tendency to decrease the accumulation of this ROS in plants grown in S1 (34%) and in S2 (41%), in comparison with their non-amended counterparts (Figure 3a). Concerning H_2O_2, significant differences were only detected between soils (Tables S3 and S4), with plants growing in S2 showing an increase up to 82% when comparing with OECD grown plants (Figure 3b). Moreover, although not statistically significant, the application of the NM lowered the levels of H_2O_2, especially in plants grown in S2 (Figure 3b). Likewise, LP was only changed in response to the type of soil (Tables S3 and S4). As documented in Figure 3c, MDA levels of S1- and S2-exposed plants were higher (S1: 28%; S2: 50%) than those grown in OECD soil, although statistical relevance was only achieved for S2.

[Figure 3]

3.7. Non-enzymatic antioxidant system – Proline, AsA and GSH

A significant interaction between the soil and the application of nano-Fe_2O_3 was found for proline levels (Tables S3 and S4). More precisely, plants grown in S2 had a higher proline content (134% increase) than those grown in S1 and OECD soil (Figure 4a). However, when S2 was amended with the NM, proline levels were reduced by 60% (Figure 4a). For the other soils, the application of nano-Fe_2O_3 did not change the accumulation of this osmolyte (Figure 4a).

The content of GSH is presented in Figure 4b and as shown, no statistical differences were observed for any of the factors (Tables S3 and S4). However, in a general way, plants exposed to S2 displayed a tendency for having higher levels of GSH, being this effect even more pronounced after the amendment with nano-Fe_2O_3.

In what regards the redox balance of AsA, its total content, as well as its reduced (AsA) and oxidized (DHA) forms, were significantly affected by both factors, but no significant interaction between them was found (Tables S3 and S4). As illustrated in Figure 4c, plants from S2 had a higher content (62%) of total AsA than those from OECD soil. Moreover, in general, the amendment of soil with nano-Fe_2O_3 further increased the levels of this antioxidant, especially in OECD (42%) and S1 (43%), in relation to the non-amended soils. Concerning the AsA and DHA ratios, significant differences were found for both forms (Tables S3 and S4) between soils and upon application of nano-Fe_2O_3. From what can be observed, AsA/Total AsA quotient was maximum in plants from S1, especially when the soil was amended with the NM, whilst the opposite was registered for DHA (Figure 4d).

[Figure 4]

3.8. Enzymatic antioxidant system – SOD, CAT and APX

The analysis of the total SOD activity revealed that this enzyme was affected by both factors, with a significant interaction between them (Tables S3 and S4). The results showed that S1-exposed plants exhibited higher activity levels (37%) than the control plants, while no change in control were detected when plants were exposed to S2 (Figure 5a). Moreover, the amendment of soil with nano-Fe_2O_3 stimulated the activity of this enzyme, especially in plants grown in S1 and S2 by 30 and 74%, respectively, in comparison with their non-amended counterparts (Figure 5a).

Regarding CAT, different responses were obtained between soils and with the NM amendment (Tables S3 and S4). As can be observed in Figure 5b, an increase of the activity of this enzyme was observed in plants exposed to S2 (almost 60% comparing with the OCDE-grown plants). In what concerns the effects of nano-Fe_2O_3, differences were observed only for OECD-grown plants (rise of 55% in amended soil) (Figure 5b).

APX activity was only changed in response to the type of soil (Tables S3 and S4), with an increase in activity of this enzyme by 62% in S2, when compared with plants grown in the artificial OECD soil (Figure 5c).

[Figure 5]

4. Discussion

4.1. Pseudo total and available contents of PTEs in soils

The levels of the studied elements were high, mainly in S2, with some of them overpassing the reference values proposed by the Portuguese Environmental Agency (APA, 2019) and the Canadian guideline values (CCME, 2007; 2018) for agricultural soils (Table 1). These results are in line with what has been reported in previous studies for soils surrounding the Estarreja Chemical Complex (Cachada et al. 2009; Reis et al. 2009; Inácio et al. 2014).

The studied soils were developed over a parent material mainly formed by beach and river terrace deposits (Cachada et al. 2009), with a sandy texture, acidic pH values and low to medium organic matter content (Table 1). These properties usually offer a reduced sorptive capacity, as shown by the extraction methods applied for evaluating the availability of PTEs. Despite the $CaCl_2$-extractable PTE contents were very low for the great majority of PTEs, a higher availability was observed when EDTA extraction was performed (Table 2). Single extraction procedures are one of the main approaches used to obtain information about metals' availability in soils and also to infer about their potential bioavailability (Rao et al. 2008; Arenas-Lago et al. 2016; Almendros et al. 2020). Weak and unbuffered salt solutions as $CaCl_2$ are usually used to mimic raining events and their contribution to remove metals that are weakly retained by electrostatic forces in organic and inorganic sites of soil components (Rao et al. 2008). Generally, this fraction accounts for less than 2% of PTEs in soils, except for some elements as Mg, Mn, and K (Emmerson et al. 2000). This was, in fact, what was recorded in our study, except for Cd and Zn in the S1. However, despite the high extraction efficiencies, the $CaCl_2$-extracted concentrations of these elements were very low (Table 2). The EDTA is a strong chelating reagent that can displace PTEs from insoluble organic and organometallic complexes, as well as those adsorbed to inorganic soil components such as oxides and clay minerals (Rao et al. 2008). Synthetic chelators as EDTA may mimic the role of many natural chelants that result from the decomposition of organic matter (e.g., organic acids and humic acids), rendering metals available to plants. Organic acids, for example, which can have different origins in soils, including being components of plant exudates, may chelate metals, modulating their cationic characteristics, and making them more available to plants (Adeleke et al. 2017). Based on this similarity as well as on positive correlations found between the content of metals in EDTA extracts and plant tissues (e.g., Gupta and Sinha, 2007; Almendros et al. 2020), this extractant has been considered representative of the metal's fractions in

soils available to plants, although it is well known that this depends on the plant species as well (e.g., Gupta and Sinha, 2007; Agrelli et al. 2020; Almendros et al. 2020). Taking this into account, the analysis of S1 and S2 EDTA-extractants suggest that some PTEs, such as Cd, Cu and Pb have more potential to become available, representing a possible risk to crop species that may be cultivated in these soils (Table 2).

4.2. The effect of nano-Fe_2O_3 on the PTEs availability and soil-plant transfer

Fe-based NMs have strong redox and sorption properties and can act as analogues of ubiquitous natural soil Fe phases, being involved in oxidation-reduction reactions with PTEs ions, formation of amorphous iron-PTEs or can simultaneously sorb both cationic (Cd, Cu, Pb or Zn) or anionic (As, Sb) elements (e.g., Komárek et al. 2013; Arenas-Lago et al. 2019; Rodríguez-Seijo et al. 2020). Although some authors showed an immobilization efficiency of studied PTEs by Fe-based NMs over 70% (e.g., Komárek et al. 2013; Gil-Díaz et al. 2016, 2017; Arenas-Lago et al. 2019; Wan et al. 2020; Rodríguez-Seijo et al. 2020), in our case, the effectiveness of the nano-Fe_2O_3 for chemical immobilization has been moderate and only recorded for Cd, Cu, Pb, Sb and Zn in S2, when EE (%) was compared between the non- and the amended soil samples (Table 2). As indicated by Gil-Díaz et al. (2016, 2017) or Rodríguez-Seijo et al. (2020), the presence of several PTEs with different chemical behavior can induce competition for sorption sites, with a reduction in immobilization efficiency for some elements. Besides, some studies with higher efficiencies were usually made with single contamination exposure or elements with similar chemical properties (e.g., Pb/Zn vs. As/Sb) - thus not mimicking element mixtures like in this study (e.g., Huang et al. 2018; Hussain et al. 2019; Rizwan et al. 2019) - artificial or metal spiked soils (e.g., Gil-Díaz et al. 2016), the use of other types of Fe-NMs (e.g., Komárek et al. 2013; Gil-Díaz et al. 2016, 2017; Wan et al. 2020), and/or higher doses of the NMs than those herein used (e.g., Gil-Díaz et al. 2014; 2016, Wan et al. 2020), that could explain these differences regarding the metal reduction efficiency. In fact, in future studies, a given percentage of nano-Fe_2O_3 should not be assumed based on previous reports, as the behavior of this NM in the soil, as well as its adsorption capabilities, may also depend on soil properties. Therefore, a pilot study similar to the one performed in this study, should be carried out, in order to determine the best dose of the hematite NMs to be applied in each case.

The amendment of the soils with the NMs also did not contribute to reducing the bioavailable content of metals in the aerial parts of plants, except for Zn in plants grown in S1 and for Sb in plants grown in S2 (Table 3). In what regards the PTEs at highest levels in the leaves of plants (As, Ba, Cu, Fe and Mn), no

significant differences were recorded between plants from non-amended and amended soils (Table 3). Sun et al. (2012) made an analysis of available ecotoxicity data and estimated HC5 values for As (hazard concentration for 5% of plant species) both based on EC_{10} and EC_{50} of 7.83 and 25.27 mg kg^{-1}, respectively. The total concentration of As found in S1 and S2 clearly surpassed these values, they were accumulated by the plants as well, and the amendment with NM did not reduce their availability. Thus, As is expected to be one of the elements involved in the phytotoxicity of these soils. Regarding Ba, a PNEC value of 314.9 mg $kg^{-1}$was proposed by ECHA for soil organisms (https://echa.europa.eu/registration-dossier/-/registered-dossier/15037/6/1) although it was highlighted by this agency that there are no reliable data for plants. Regarding Cu, Caetano et al. (2016) recorded EC50 values for plants varying between 89 and 290.5 mg kg^{-1}. Only the pseudo-total concentration of this PTE surpassed this toxicity thresholds.

Barley plants have defense mechanisms to reduce or limit the transfer of PTEs from the soil to the aerial part. This so-called root barrier could explain why no differences in the studied elements were observed between non-amended and amended soils with nano-Fe_2O_3 (Soriano-Disla et al. 2014). In this study, the concentration of Fe in the leaves was not changed in both soils after amendment with hematite (Table 3), which indicates that Fe added to soils in the nano form, was not up taken and translocated by the roots of plants to the aerial parts as indicated by other researchers for nano-Fe_3O_4 amendment (Tombuloglu et al. 2017; de Souza et al. 2019). However, more analyses, such as transmission electron microscopy, should be carried out to assess the potential root-to-shoot translocation of this NM.

4.3. Nano-Fe_2O_3 improves the growth performance and physiological status of barley plants exposed to S1 and S2 soils

The results herein obtained point towards a toxic effect of both studied soils (S1 and S2) on plant growth and development, when compared to plants grown in the OECD artificial soil. For all parameters studied, inhibition values up to 75% were recorded for roots and leaves (Figure 1), unequivocally suggesting the phytotoxicity of these soils, with the observed effects being dependent not only on the degree of contamination of the tested soils, but also on the mixture effects and/or the characteristics of the soil itself. Although PTEs are identified as more hazardous (As, Cu, Pb, and Zn), with high concentrations especially in S2, they can quickly induce toxicity both at the macroscopic and cellular level (Seneviratne et al. 2017; Singh et al. 2016), it must be highlighted that, for S1, the recorded phytotoxicity may arise not only from the presence of these mixtures of PTEs, but also from the low pH of the soil (pH < 5), and its low organic

matter content (<3.4% OM) (Zdruli et al. 2004), within other properties or contaminants that were not analysed in this study. The problems associated to soil acidity can be linked to scenarios of nutrient deficiency (namely P, and Mg), which is unlikely to happened here given the recorded values of these elements in S1-exposed plants, or metal toxicity (especially Mn and Al). In fact, it is known that, under pH < 5.5, the mobility and solubility of Al is increased, occurring mainly as Al^{3+}, its most phytotoxic form, which greatly impacts plant growth and development (Wang et al. 2006). Curiously, among all cereals, barley is the most susceptible species to Al toxicity (Ma et al. 2014; Wang et al. 2006). Thus, although there might be other factors (e.g., PTEs mixture effects and low organic matter content) behind S1-mediated toxicity in *H. vulgare*, the effects of Al and acidity may have also played an important role.

Despite the high degree of phytotoxicity recorded, when soils were amended with nano-Fe_2O_3, the growth performance of barley plants was stimulated in comparison with the non-amended soils, especially in S1 (Figure 1). Besides being an essential micronutrient, thereby contributing to a better nutritional status, it is recognized that Fe can act as a metal scavenger, reducing the uptake of PTEs. Indeed, in line with the findings of the current study, the application of nano-Fe_2O_3 was found to improve plant abiotic stress tolerance, mitigating metal phytotoxicity (Konate et al. 2017; Hussain et al. 2019).

As reviewed by Zuverza-Mena et al. (2017), Fe-based nanomaterials are barely up taken by plants, being assumed to remain in the soil, given their insolubility and adherence to soil particles. Therefore, it can be hypothesized that the recorded positive influence of nano-Fe_2O_3 in barley growth is much likely related to the behavior and influence of the NM on soil properties and element availability rather than on its uptake and effects on roots and shoots. Indeed, it has been demonstrated that NM exceeding 20 nm cannot penetrate the cell walls (Rico et al. 2013, Martínez-Fernández et al. 2016, Zuverza-Mena et al. 2017), being their effects strongly linked to particle aggregation on the root surface and their binding to cation exchange sites (Trakal et al. 2015). In line with this premise, leaf levels of Fe did not change upon nano-Fe_2O_3 application on S1 and S2, though an increment was observed in plants grown in OECD soil (Table 3). Several explanations could be hypothesized to explain this result, but any of them could be confirmed. However, when comparing plants from all the soils (without the amendment), it is possible to see that those grown in the OECD soil had the lowest Fe levels in the leaves. The scarcity of Fe in OECD soil and the addition of hematite to the soils may have triggered deeply studied biochemical reactions and mechanisms which evolved in plants to make iron available for uptake (Connorton et al. 2017). Furthermore, and supporting our main hypothesis – that Fe is acting as nano-adsorbent for many PTEs – the available fraction

438 of Fe ions to be uptaken by plants is reduced in the contaminated soils (S1 and S2) than in OECD, which
439 can partially explain the higher levels of Fe in OECD soil-grown plants. Moreover, other soil properties,
440 such as pH and OM, could have also played a role in this phenomenon.

441 As important as understanding the role of nano-Fe_2O_3 in enhancing the growth of PTEs-exposed
442 plants, it is to perceive and unravel how the redox homeostasis of exposed plants is modulated. One of the
443 most common symptoms of PTEs phytotoxicity is the occurrence of tissue chlorosis, suggestive of pigment
444 losses (Sharma et al., 2019; 2020a). Here, barley plants exposed to S1 and S2 exhibited leaf chlorosis,
445 especially in the younger leaves (data not shown). In fact, it has been shown that several metals are able to
446 affect photosynthesis in different dimensions, inducing changes from the molecular and biochemical levels
447 to the functional and metabolic ones (Paunov et al., 2018). Despite carotenoid levels remained unchanged
448 among treatments, our data showed that both test soils led to reductions of chlorophylls content, being this
449 reduction more accentuated in plants exposed to S2 (Figure 2). In fact, and as an example, As is known to
450 reduce the photosynthetic yield, lowering the chlorophyll levels, and hampering the electron transport chain
451 and photosystem II activity (Finnegan and Chen 2012). Losses in chlorophyll content are usually
452 accompanied by a deregulation of the whole photosynthetic process, culminating in great metabolic
453 disorders with pronounced consequences for plant growth (Sharma et al., 2019). With effect, metals have
454 been found to reduce the number and size of chloroplasts and to inhibit the biosynthesis of chlorophylls,
455 especially by degrading their biosynthetic enzymes (Sharma et al. 2019; 2020b)

456 Regarding nano-Fe_2O_3 application, no differences were registered between non- and amended soils,
457 though a tendency for increased chlorophyll values was noticed when plants were exposed to the NM
458 amended soils. However, based on the hypothesis that NMs were not able to reach, at least substantially,
459 the aerial parts of the plants, the partial recovery of chlorophylls is not directly related to Fe's role, but
460 rather to other induced metabolic adjustments, namely a more balanced nutrient uptake and reduced PTEs
461 accumulation. Actually, and corroborating this hypothesis, the amendment of S1 with nano-Fe_2O_3 resulted
462 in a slight increase in nutrients bioavailability (Table 2), probably due to an increment of soil pH after NMs
463 amendment. Indeed, the pH of S1 increased to 5.9 upon nano-Fe_2O_3 amendment, concomitant with a
464 significant decrease in Al toxicity and in the PTEs availability, possibly explaining the better growth
465 performance of barley recorded in S1 amended with the NMs (Table 2). Previous studies conducted with
466 Fe oxides NMs also reported an increase of soil pH upon soil amendments (e.g. Gil-Díaz et al. 2014; 2017;
467 2018; Rodríguez-Seijo et al. 2020), lowering the phytotoxicity of PTEs to common vetch, barley and wheat

(e.g. Gil-Díaz et al. 2014, 2018; Rizwan et al. 2019) and the immobilization of some metal cations, such as Pb ions, through processes of ion exchange and surface complexation (Gil-Díaz et al. 2014; 2018; Arenas-Lago et al. 2019; Rodríguez-Seijo et al. 2020).

4.4. Oxidative stress markers

The occurrence of oxidative stress is one of the most preserved and common responses to all types of abiotic stress (reviewed by Soares et al. 2019a). Therefore, the evaluation of different components of the redox metabolic pathways can provide objective clues on the cellular state upon exposure to adverse growth conditions, like soil degradation by PTEs contamination (Figure 3). Although in general both S1 and S2 induced the accumulation of ROS in barley plants in comparison with the OECD soil, subtle differences were recorded between the two contaminated soils. While in S1 only H_2O_2 was increased, in S2 both analyzed ROS were enhanced in leaves of barley plants (Figure 3). These differences may arise because of the differences between both soils, since S2 shows a higher contamination degree than S1. Even though ROS production can result from the interference of the metallic ions with several electron transport chains (ETC), especially those present in chloroplasts and mitochondria, the overproduction of ROS induced by PTEs is dependent on different factors, including the concentration of the element itself (Shahid et al. 2014), as well as possible synergistic or antagonistic effects. Concomitantly to this overproduction of ROS, the levels of MDA increased upon exposure to S1 and S2 (Figure 3), strongly indicating the consequent induction of oxidative stress effects in leaves of barley plants grown under PTEs excess, as observed in previous studies (Soares et al. 2016, 2018; Sousa et al. 2020,). Actually, and recalling the excessive levels of some of these PTEs in S1 and S2, the observed redox disbalance was not surprising. In fact, although a multi-contaminated soil can lead to distinct effects compared to those caused by individual PTEs, the involvement of As, Cu, Pb and Zn in inducing oxidative disturbances in plant cells is well-documented (e.g., Branco-Neves et al. 2017; Kostecka-Gugała and Latowski 2018; Lin and Aarts 2012; Ravet and Pilon 2013; Sousa et al. 2020), and their single and combined effects can translate into oxidative stress in plants.

Given the positive influence of nano-Fe_2O_3 on the growth performance of barley exposed to S1 and S2, it was hypothesized that the application of these NM could decrease the oxidative stress imposed by PTEs in plant cells. Accordingly, although not always statistically meaningful, the presence of nano-Fe_2O_3 in the soil helped to reduce the overproduction of ROS, especially in S2, where the maximum damage was recorded (Figure 3). As can be observed, in S1, a tendency of decreasing levels of $O_2^{\cdot-}$, H_2O_2 and LP was found, suggesting a positive effect of nano-Fe_2O_3 amendment in S1. In parallel, despite LP did not change

498 in response to the NM amendment, levels of both ROS were diminished in leaves of plants grown in S2
499 previously amended with nano-Fe_2O_3 (Figure 3). In agreement, the supplementation of nano-Fe_2O_3 to the
500 nutritive medium helped to reduce the oxidative damage induced by As in *Brassica juncea* (L.) Czern.,
501 limiting the occurrence of LP (Praveen et al. 2018). Furthermore, Hussain et al. (2019), in a study conducted
502 with *Triticum aestivum* L., also reported that nano-Fe_2O_3, applied as a foliar spray or added to the soil, was
503 able to reduce Cd-induced oxidative stress, lowering the electrolyte leakage of biological membranes.
504 Despite no PTEs' bioaccumulation was observed (Table 3) at the leaf level, the application of nano-Fe_2O_3
505 showed beneficial effects recorded on oxidative stress biomarkers, suggesting that they are somehow
506 contributing for better plant growth performance, especially in contaminated soils. Actually, it has been
507 shown that Cu and Zn oxide NMs can cause significant changes in roots, which further translate in modified
508 transcriptional patterns related to metal-tolerance in shoots, where NP were not detected in their surfaces
509 (Anderson et al. 2017). Moreover, other hypothesis that cannot be completely excluded is the potential of
510 nano-Fe_2O_3 to reduce the bioaccumulation of PTEs in the root tissues, thereby promoting a better growth
511 and physiological performance of barley plants. Though this data would be important, methodologies
512 providing real and feasible results concerning the fraction of PTEs adsorbed to the root tissue or
513 bioaccumulated are difficult to implement, given that a considerable amount of soil particles and NMs can
514 remain adsorbed to the root system, being hard to evaluate with accuracy the fraction of PTEs really
515 accumulated by plant roots.

516 *4.5. Response of the plant antioxidant system*

517 In order to overcome constant fluctuations of the abiotic environment and to face biotic interactions, plants
518 have developed an efficient antioxidant system, composed by enzymatic and non-enzymatic players that
519 act synergistically to counteract the toxic effects of ROS (as reviewed by Soares et al. 2019a). Thus, when
520 evaluating the potential of nano-Fe_2O_3 to reduce the phytotoxicity of metal-contaminated soils, it is also
521 important to analyze the antioxidant response, either by the direct quantification of several metabolites,
522 such as proline, GSH, and AsA, but also by the evaluation of the catalytic action of important enzymes, as
523 SOD, CAT, and APX.

524 Proline, a proteinogenic amino acid formerly known as an active osmolyte, is now also considered as
525 a powerful antioxidant, which accumulates in plant cells under stressful conditions (Soares et al. 2019a).
526 Proline can serve as a metal chelator and is able to stimulate the synthesis of other important compounds,
527 such as phytochelatins (Hayat et al. 2012). Our results showed that proline accumulation did not change

when plants were exposed to S1, however, a substantial increase of its levels was detected upon exposure to S2, strengthening the premise that this soil shows a higher phytotoxic potential than S1 (Figure 4). Furthermore, since proline can act as a membrane stabilizer, it can be suggested that the observed increase of its content was not enough to neutralize the toxic effects of ROS on lipid peroxidation, whose levels remained higher in the leaves of plants grown in S2. Once again, the addition of nano-Fe_2O_3 to S2 was also found to alleviate the observed toxicity, since proline levels decreased to values identical to those found in plants grown in OECD soil. Accordingly, Praveen et al. (2018) reported that As-induced overaccumulation of proline was reduced by the application of nano-Fe_3O_4.

Besides proline, AsA and GSH are two of the most relevant plant antioxidants, capable of directly interacting with ROS and/or serving as substrates for different antioxidant enzymes. The results revealed that GSH did not majorly change upon treatments, though a tendency for plants grown in S2 to exhibit increased values of this metabolite was found. As in the case of GSH, AsA cellular homeostasis depends on the balance between its reduced (AsA) and oxidized (DHA) forms. As can be seen, both studied soils contributed to the accumulation of this antioxidant in leaves of *H. vulgare*, being this increased content related to a higher abundance of AsA in comparison with DHA. Indeed, it is known that both AsA and GSH function as cellular buffers, contributing to the maintenance of the cellular redox balance (Soares et al. 2019a).

Over the last years, the involvement of several metal oxide NMs on the stimulation of the plant antioxidant system has been described (Soares et al. 2018a, 2018b). Here, upon application of nano-Fe_2O_3, levels of AsA were further enhanced when compared to the non-amended soils, with an even higher proportion of AsA in relation to DHA (Figure 4). This observation suggests a higher ability of plants grown under NM-amended soils to enhance their antioxidant potential to minimize the phytotoxic effects of both S1 and S2. Moreover, knowing that AsA is capable of directly neutralize H_2O_2, it can also be suggested that the observed decreased values of this ROS can be related to the antioxidant activity of AsA. Indeed, more than being APX's substrate, AsA is described as the most powerful antioxidant in plants, playing multiple roles in the redox system, namely on ROS scavenging (Soares et al. 2019a).

In what concerns the enzymatic component of the plant antioxidant system, an integrative insight into the main antioxidant enzymes was performed. Leaves of barley plants grown in S1 showed increased activity of SOD, but neither CAT nor APX were affected; on the other hand, SOD remained unchanged in plants exposed to S2, but the activity of CAT and APX was significantly enhanced (Figure 5). When

558 discussing the involvement of these three enzymes in the cellular redox homeostasis, it is important to take
559 a look at the measured levels of $O_2^{\cdot-}$ and H_2O_2. Indeed, while SOD, considered as the first enzymatic line
560 of the antioxidant defense system, is responsible for the dismutation of $O_2^{\cdot-}$ into H_2O_2 and O_2, both CAT
561 and APX play important role in H_2O_2 cellular detoxification (Soares et al. 2019a). Thus, the tendency for
562 S1-exposed plants to exhibit lower values of $O_2^{\cdot-}$ is much likely related to the higher activity of SOD; in
563 contrast, since SOD did not change in S2-exposed plants, the levels of $O_2^{\cdot-}$ were kept high (Figures 3 and
564 5). Regarding H_2O_2, the observed rise of its levels in plants grown in S1 can be a result of the maintenance
565 of CAT and APX activity, while in S2-exposed plants, the increment of these two enzymes was not enough
566 to prevent the overaccumulation of this ROS (Figures 3 and 5). The modulation of enzyme activity by stress
567 factors, including PTEs and soil acidity/alkalinity, is well described in the literature, being recognized that
568 both stress (e.g., type of stressor, magnitude, repeated exposures) and genotype characteristics can lead to
569 distinct effects on enzymes' performance (Soares et al. 2019a).

570 The effects of nano-based formulations of Fe on the antioxidant system are barely known and require
571 additional studies. In the current study, SOD activity was found to be positively affected by the application
572 of nano-Fe_2O_3, since increased levels of activity of this enzyme were found in leaves of plants grown under
573 contaminated soils amended with the NM. In parallel, a recent work with wheat seedlings found that SOD
574 activity was enhanced upon application of nano-Fe_3O_4 (2000 mg L^{-1}), ameliorating the toxic effects
575 imposed by different metals (1 mM) supplemented to the nutrient solution (Konate et al. 2017). This finding
576 is quite curious and may reflect the role of nano-Fe_2O_3 in modulating Fe metabolism in plants, probably
577 stimulating enzymes that use this element as co-factor, such as Fe-SOD. However, it should not be
578 discarded that the upregulation of SOD in plants exposed to the NM can also be the result of other isoforms
579 of the enzyme, differing in the metal present in its active site, such as Cu/Zn- and Mn-SOD. Regarding
580 CAT and APX, in general, the addition of nano-Fe_2O_3 to S1 and S2 did not majorly change their activity
581 patterns (Figure 5), revealing that, at least under the experimental conditions herein described, nano-Fe_2O_3
582 did not contribute for a better performance of these two antioxidants enzymes.

583 The application of nano-Fe_2O_3 to metal-contaminated soils allowed to reduce, at least to some extent,
584 the phytotoxic effects on the growth of barley plants. Moreover, physiological and biochemical analyses
585 showed that both tested soils, especially S2, imposed a severe oxidative stress condition in *H. vulgare*, by
586 the overproduction of ROS and subsequent induction of LP in the leaves; however, soil amendment with

nano-Fe_2O_3, by preventing PTEs toxicity and altering soil properties (e.g., pH), contributed for a better performance of the plant antioxidant system, thereby reducing the degree of oxidative damage.

In conclusion, this work provides practical knowledge on the use of iron-based NMs to alleviate the toxicity of PTEs in multi-contaminated agricultural soils as an effective and sustainable tool to enhance plant productivity under adverse growth conditions in soils with their production function impaired. In the future, studies should explore the effects of other types and concentrations of NMs on the modulation of soil properties and functions, giving particular attention to the impacts on relevant crop species, including monocot and dicot plants, and studies with longer exposure periods.

Supplementary Materials: Figure S1 and Tables S1-S4

Data availability: All data generated or analyzed during this study are included in this article.

Author Contributions: Conceptualization, A.R.S., C.S., F.F., R.P., A.C.; methodology, C.S., A.R.S., F.F., A.C., R.P., CP; formal analysis, C.S., A.R.S., A.C., CP., S.R., B.F.A; investigation, C.S., A.R.S, S.R., B.F.A., C.P., A.C.; resources, A.R.S., C.P., A.C., F.F., R.P.; writing—original draft preparation, C.S., A.R.S., S.R., B.F.A.; writing—review and editing, C.S., A.R.S., A.C., F.F., R.P; supervision, A.R.S., C.S., F.F., R.P.; project administration, R.P.; funding acquisition, A.R.S, C.P., A.C., F.F., R.P.

Funding: This research has been (co)funded by the LabEx DRIIHM, French programme "Investissements d'Avenir" (ANR-11-LABX-0010) which is managed by the ANR within the Observatoire Hommes-Milieux Estarreja (OHM-E/2017/Proj.3). This research was supported by the Strategic Funding UIDB/04423/2020 and UIDP/04423/2020 (CIIMAR), UIDB/05748/2020 and UIDP/05748/2020 (GreenUPorto), and UID/GEO/04035/2020 (GEOBIOTEC) through national funds provided by the Portuguese Foundation for Science and Technology (FCT) and MCTES and the co-funding by the FEDER, within the PT2020 Partnership Agreement and Compete 2020. CS acknowledges the support by grant SFRH/BD/115643/2016 from FCT. ARS and AC would like to acknowledge the FCT and CIIMAR for their individual research contracts (CEECIND/03794/2017 and CEECIND/00058/2017, respectively).

Acknowledgements: A.R.S. also acknowledges the donation of nanomaterials and technical support to Maria Luisa Andrade Couce, Flora Alonso Vega, Manoel Lago-Vila, and Daniel Arenas-Lago.

References

Adeleke, R., Nwangburuka, C., Oboirien, B., 2017. Origins, roles and fate of organic acids in soils: A review. S. Afr. J. Bot. 108, 393-406. https://doi.org/10.1016/j.sajb.2016.09.002

Aebi, H., 1984. Catalase *in vitro*. Meth. Enzimol. 105, 121-126. https://doi.org/10.1016/S0076-6879(84)05016-3

Agrelli, D., Caporale, A.G., Adamo, P., 2020. Assessment of the Bioavailability and Speciation of Heavy Metal(loid)s and Hydrocarbons for Risk-Based Soil Remediation. Agronomy 10, 1440. https://doi.org/10.3390/agronomy10091440

Almendros, P., González, D., Ibañez, M.A., Fernández, M.D., García-Gómez, C., et al., 2020. Can Diffusive Gradients in Thin Films (DGT) Technique and Chemical Extraction Methods Successfully Predict both Zn Bioaccumulation Patterns in Plant and Leaching to Groundwater in Soils Amended with Engineered ZnO Nanoparticles?. J. Soil Sci. Plant Nutr. 20, 1714–1731. https://doi.org/10.1007/s42729-020-00241-x

Anderson, A.J., McLean, J.E., Jacobson, A.R., Britt, D.W., 2017. CuO and ZnO nanoparticles modify interkingdom cell signaling processes relevant to crop production. J. Agric. Food Chem. 66(26), 6513-6524. https://doi.org/10.1021/acs.jafc.7b01302

APA, 2019. Solos Contaminados – Guia Técnico. Valores de Referência para o Solo. Agência Portuguesa do Ambiente. Lisbon 2019. https://apambiente.pt/index.php?ref=16&subref=1479&sub2ref=1535 *In portuguese* (accessed 25.10.20)

Arenas-Lago, D., Rodríguez-Seijo, A., Lago-Vila, M., Andrade, M.L., Vega, F.A., 2016. Using $Ca_3(PO_4)_2$ nanoparticles to reduce metal mobility in shooting range soils. Sci. Total Environ. 571, 1136-1146. https://doi.org/10.1016/j.scitotenv.2016.07.108

Arenas-Lago, D., Abreu, M.M., Andrade, M.L., Vega, F.A., 2019. Is nanoremediation an effective tool to reduce the bioavailable As, Pb and Sb contents in mine soils from Iberian Pyrite Belt?. Catena 176, 362-371. https://doi.org/10.1016/j.catena.2019.01.038

Bates, L.S., Waldren, R.P., Teare, I.D., 1973. Rapid determination of free proline for water-stress studies. Plant Soil 39, 205–207 https://doi.org/10.1007/BF00018060

646 Batista, A.C., Ferreira da Silva, E., Azevedo, M.C.C., Sousa, A.J., Cardoso Fonseca, E., 2002. Soil data
647 analysis from central Portugal by Principal Component Analysis and geostatistical techniques. Geochem.:
648 Explor. Environ. Anal. 2(1), 15-25. https://doi.org/10.1144/1467-787302-002
649 Bradford, M.M., 1976. A rapid and sensitive method for the quantitation of microgram quantities of protein
650 utilizing the principle of protein-dye binding. Anal. Biochem. 72(1-2), 248-254.
651 https://doi.org/10.1016/0003-2697(76)90527-3
652 Branco-Neves, S., Soares, C., Sousa, A., Martins, V., Azenha, M., Gerós, H., Fidalgo, F., 2017. An efficient
653 antioxidant system and heavy metal exclusion from leaves make *Solanum cheesmaniae* more tolerant to
654 Cu than its cultivated counterpart. Food Energy Secur. 6, 123-133. https://doi.org/10.1002/fes3.114
655 British Standards, 2000. BS EN 13039:2000. Soil improvers and growing media. Determination of organic
656 matter content and ash. British Standards Institution, London, 2000.
657 Cachada, A., Rodrigues, S.M., Mieiro, C., Ferreira da Silva, E., Pereira, E., Duarte, A.C., 2009. Controlling
658 factors and environmental implications of mercury contamination in urban and agricultural soils under a
659 long-term influence of a chlor-alkali plant in the North–West Portugal. Environ. Geol. 57, 91.
660 https://doi.org/10.1007/s00254-008-1284-2
661 Caetano, A.L., Marques, C.R., Gonçalves, F., Ferreira da Silva, E., Pereira, R., 2016. Copper toxicity in a
662 natural reference soil: ecotoxicological data for the derivation of preliminary soil screening values.
663 Ecotoxicology 25, 163–177. https://doi.org/10.1007/s10646-015-1577-7
664 CCME, 2007. Canadian Soil Quality Guidelines for the Protection of Environmental and Human Health
665 Canadian Council of Ministers of the Environment, Winnipeg.
666 CCME, 2018. Canadian soil quality guidelines for the protection of environmental and human health.
667 Canadian Council of Ministers of the Environment, Winnipeg. Available at
668 https://www.ccme.ca/en/resources/canadian_environmental_quality_guidelines/index.html (accessed
669 25.10.20)
670 Connorton, J.M., Balk, J., Rodríguez-Celma, J., 2017. Iron homeostasis in plants - a brief overview.
671 Metallomics 9(7), 813-823. http://doi.org/10.1039/c7mt00136c
672 Costa, C., Jesus-Rydin, C., 2001. Site investigation on heavy metals contaminated ground in Estarreja —
673 Portugal. Eng. Geol. 60, 1-4, 39-47. https://doi.org/10.1016/S0013-7952(00)00087-9

de Souza, A., Govea-Alcaide, E., Masunaga, S.H., Fajardo-Rosabal, L., Effenberger, F., Rossi, L.M., Jardim, R.F., 2019. Impact of Fe_3O_4 nanoparticle on nutrient accumulation in common bean plants grown in soil. SN Appl. Sci. 1, 308. https://doi.org/10.1007/s42452-019-0321-y

Donahue, J.L., Okpodu, C.M., Cramer, C.L., Grabau, E.A., Alscher, R.G., 1997. Responses of Antioxidants to Paraquat in Pea Leaves (Relationships to Resistance). Plant Physiol. 113(1), 249-257. https://doi.org/10.1104/pp.113.1.249

Emmerson, R.H., Birkett, J.W., Scrimshaw, M., Lester, J.N., 2000. Solid phase partitioning of metals in managed retreat soils: field changes over the first year of tidal inundation. Sci. Total Environ. 254(1), 75-92. https://doi.org/10.1016/s0048-9697(00)00442-3

Feng, M.H., Shan, X.Q., Zhang, S., Wen, B., 2005. A comparison of the rhizosphere-based method with DTPA, EDTA, $CaCl_2$, and $NaNO_3$ extraction methods for prediction of bioavailability of metals in soil to barley. Environ. Pollut. 137(2), 231-40. http://doi.org/10.1016/j.envpol.2005.02.003

Finnegan, P., Chen, W., 2012. Arsenic toxicity: the effects on plant metabolism. Front. Physiol. 3, 182 https://doi.org/10.3389/fphys.2012.00182

Foyer, C.H., Noctor, G., 2011. Ascorbate and glutathione: the heart of the redox hub. Plant Physiol. 155(1), 2-18. https://doi.org/10.1104/pp.110.167569

Gajewska, E., Skłodowska, M., 2007. Effect of nickel on ROS content and antioxidative enzyme activities in wheat leaves. Biometals 20, 27-36. https://doi.org/10.1007/s10534-006-9011-5

García-Gómez C, Obrador A, González D, Babín M, Fernández MD., 2018 Comparative study of the phytotoxicity of ZnO nanoparticles and Zn accumulation in nine crops grown in a calcareous soil and an acidic soil. Sci. Total Environ. 644, 770-780. http://doi.org/10.1016/j.scitotenv.2018.06.356

Gee GW, Bauder JW., 1986. Particle size analysis. In: Klute A (Ed.). Methods of soil analysis, part I, 2nd ed., Madison: American Society of Agronomy Inc; pp. 383-409. https://doi.org/10.2136/sssabookser5.1.2ed.c15

Gil-Díaz, M., Pérez-Sanz, A., Ángeles Vicente, M. and Carmen Lobo, M., 2014. Immobilisation of Pb and Zn in Soils Using Stabilised Zero-valent Iron Nanoparticles: Effects on Soil Properties. Clean Soil Air Water, 42, 1776-1784. https://doi.org/10.1002/clen.201300730

Gil-Díaz, M., González, A., Alonso, J., Lobo, M.C., 2016. Evaluation of the stability of a nanoremediation strategy using barley plants. J. Environ. Manage. 165, 150-158. https://doi.org/10.1016/j.jenvman.2015.09.032

704 Gil-Díaz, M., Pinilla, P., Alonso, J., Lobo, M.C., 2017. Viability of a nanoremediation process in single or
705 multi-metal(loid) contaminated soils. J. Hazard. Mater. 321, 812-819.
706 https://doi.org/10.1016/j.jhazmat.2016.09.071
707 Gil-Díaz, M., López, L.F., Alonso, J., Lobo, M.C., 2018. Comparison of Nanoscale Zero-Valent Iron,
708 Compost, and Phosphate for Pb Immobilization in an Acidic Soil. Water Air Soil Pollut. 229, 315.
709 https://doi.org/10.1007/s11270-018-3972-1
710 Gillespie, K., Ainsworth, E., 2007. Measurement of reduced, oxidized and total ascorbate content in plants.
711 Nat. Protoc. 2, 871–874 https://doi.org/10.1038/nprot.2007.101
712 Gupta, A., Sinha, S., 2007. Assessment of single extraction methods for the prediction of bioavailability of
713 metals to *Brassica juncea* L. Czern. (var. Vaibhav) grown on tannery waste contaminated soil. J. Hazard.
714 Mater. 149(1), 144-150. https://doi.org/10.1016/j.jhazmat.2007.03.062
715 Hayat, S., Hayat, Q., Alyemeni, M.N-, Wani, A.S., Pichtel, J., Ahmad, A., 2012. Role of proline under
716 changing environments: a review. Plant Signal Behav. 7(11), 1456-1466.
717 http://doi.org/10.4161/psb.21949
718 Heat, R.L., Packer, L., 1968. Photoperoxidation in isolated chloroplasts: I. Kinetics and stoichiometry of
719 fatty acid peroxidation. Arch. Biochem. Biophys. 125, 189-198. https://doi.org/10.1016/0003-
720 9861(68)90654-1
721 Houba, V.J.G., Temminghoff, E.J.M., Gaikhorst, G.A., van Vark, W., 2000. Soil analysis procedures using
722 0.01 M calcium chloride as extraction reagent. Commun. Soil Sci. Plant Anal. 31, 1299-1396.
723 http://doi.org/10.1080/00103620009370514
724 Huang, D., Qin, X., Peng, Z., Liu, Y., Gong, X., Zeng, G., Huang, C., et al., 2018. Nanoscale zero-valent
725 iron assisted phytoremediation of Pb in sediment: Impacts on metal accumulation and antioxidative
726 system of *Lolium perenne*. Ecotox. Environ. Saf. 153, 229-237
727 https://doi.org/10.1016/j.ecoenv.2018.01.060
728 Hussain, A., Ali, S., Rizwan, M., Rehman, M.Z., Javed, M.R., Imran, M., Chatha, S.A.S, et al., 2018. Zinc
729 oxide nanoparticles alter the wheat physiological response and reduce the cadmium uptake by plants.
730 Environ. Pollut. 242, 1518-1526. https://doi.org/10.1016/j.envpol.2018.08.036
731 Hussain, A., Ali, S., Rizwan, M., Rehman, M.Z., Farooq Qayyum, M., Wang, H., Rinkbele, J., 2019.
732 Responses of wheat (T*riticum aestivum*) plants grown in a Cd contaminated soil to the application of iron
733 oxide nanoparticles. Ecotox. Environ. Saf. 173, 156-164 https://doi.org/10.1016/j.ecoenv.2019.01.118

734 Inácio, M., Neves, O., Pereira, V., Ferreira da Silva, E., 2014. Levels of selected potential harmful elements
735 (PHEs) in soils and vegetables used in diet of the population living in the surroundings of the Estarreja
736 Chemical Complex (Portugal). Appl. Geochem. 44, 38-44.
737 https://doi.org/10.1016/j.apgeochem.2013.07.017
738 ISO (2012) Soil Quality — Effects of Pollutants on Earthworms — Part 2: Determination of Effects on
739 Reproduction of *Eisenia fetida/Eisenia andrei* ISO 11268-2, Geneva, Switzerland.
740 Jana, S., Choudhuri, M.A., 1982. Glycolate metabolism of three submersed aquatic angiosperms during
741 ageing. Aquatic Bot. 12, 345-354. https://doi.org/10.1016/0304-3770(82)90026-2
742 Komárek, M., Vaněk, A., Ettler, V., 2013. Chemical stabilization of metals and arsenic in contaminated
743 soils using oxides – A review. Environ. Pollut. 172, 9-22 https://doi.org/10.1016/j.envpol.2012.07.045
744 Konate, A., He, X., Zhang, Z., Ma, Y., Zhang, P., Alugongo, G. M., et al., 2017. Magnetic (Fe_3O_4)
745 nanoparticles reduce heavy metals uptake and mitigate their toxicity in wheat seedling. Sustainability
746 9(5), 790. https://doi.org/10.3390/su9050790
747 Kostecka-Gugała, A., Latowski, D., 2018. Arsenic-Induced Oxidative Stress in Plants. In: Hasanuzzaman
748 M., Nahar K., Fujita M. (Eds.). Mechanisms of Arsenic Toxicity and Tolerance in Plants. Springer,
749 Singapore. pp 79-104 https://doi.org/10.1007/978-981-13-1292-2_4
750 Lichtenthaler, H.K., 1987. Chlorophylls and carotenoids: Pigments of photosynthetic biomembranes.
751 Methods Enzymol. 148, 350-382. https://doi.org/10.1016/0076-6879(87)48036-1
752 Lin, Y.F., Aarts, M.G., 2012. The molecular mechanism of zinc and cadmium stress response in plants.
753 Cell. Mol. Life Sci. 69, 3187–3206. https://doi.org/10.1007/s00018-012-1089-z
754 Ma, J. F., Chen, Z. C., Shen, R. F., 2014. Molecular mechanisms of Al tolerance in gramineous plants.
755 Plant Soil 381(1), 1-12. https://doi.org/10.1007/s11104-014-2073-1
756 Martínez-Fernández, D., Vítková, M., Bernal, M.P., Komárek, M., 2015. Effects of Nano-maghemite on
757 Trace Element Accumulation and Drought Response of *Helianthus annuus* L. in a Contaminated Mine
758 Soil. Water Air Soil Pollut. 226, 101. https://doi.org/10.1007/s11270-015-2365-y
759 Nakano, Y., Asada, K., 1981. Hydrogen peroxide is scavenged by ascorbate-specific peroxidase in spinach
760 chloroplasts. Plant Cell Physiol. 22(5), 867-880 https://doi.org/10.1093/oxfordjournals.pcp.a076232
761 OECD, 2006. OECD Test No. 208: Terrestrial Plant Test: Seedling Emergence and Seedling Growth Test.
762 OECD Publishing, Paris. https://doi.org/10.1787/20745761

763 Panagos, P., Van Liedekerke, M., Yigini, Y., Montanarella, L., 2013. Contaminated sites in Europe: review
764 of the current situation based on data collected through a European network. J. Environ. Public Health
765 2013, 158764 https://doi.org/10.1155/2013/158764
766 Paunov, M., Koleva, L., Vassilev, A., Vangronsveld, J., Goltsev, V., 2018. Effects of Different Metals on
767 Photosynthesis: Cadmium and Zinc Affect Chlorophyll Fluorescence in Durum Wheat. Int. J. Mol. Sci.
768 19, 787. https://doi.org/10.3390/ijms19030787
769 Pereira, M.E., Lillebø, A.I., Pato, P., Válega, M., Coelho, J.P., Lopes, C.B., et al., 2009. Mercury pollution
770 in Ria de Aveiro (Portugal): a review of the system assessment. Environ. Monit. Assess. 155, 39.
771 https://doi.org/10.1007/s10661-008-0416-1
772 Praveen, A., Khan, E., Perwez, M., Sardar, M., Gupta, M., 2018. Iron oxide nanoparticles as nano-
773 adsorbents: a possible way to reduce arsenic phytotoxicity in Indian mustard plant (*Brassica juncea* L.).
774 J. Plant Growth Regul. 37(2), 612-624. https://doi.org/10.1007/s00344-017-9760-0
775 Quevauviller, Ph., 1998. Operationally defined extraction procedures for soil and sediment analysis I.
776 Standardization. TrAC, Trends Anal. Chem. 17(5), 289-298. https://doi.org/10.1016/S0165-
777 9936(97)00119-2
778 Rao, C.R.M., Sahuquillo, A. Sanchez, J.L. 2008. A review of the different methods applied in
779 environmental geochemistry for single and sequential extraction of trace elements in soils and related
780 materials. Water Air Soil Pollut. 189(1-4), 291-333. https://doi.org/10.1007/s11270-007-9564-0
781 Ravet, K., Pilon, M., 2013.Copper and Iron Homeostasis in Plants: The Challenges of Oxidative Stress.
782 Antioxid Redox Signal. 19(9), 919–932. https://doi.org/10.1089/ars.2012.5084
783 Reis, A.T., Rodrigues, S.M., Araújo, C., Coelho, J.P., Pereira, E., Duarte, A.C., 2009. Mercury
784 contamination in the vicinity of a chlor-alkali plant and potential risks to local population. Sci. Total
785 Environ. 407, 2689-2700. https://doi.org/10.1016/j.scitotenv.2008
786 Rico, C.M., Morales, M.I., Barrios, A.C., McCreary, R., Hong, J., Lee, W.Y., et al. 2013. Effect of cerium
787 oxide nanoparticles on the quality of rice (*Oryza sativa* L.) grains. J. Agric. Food Chem. 61(47), 11278-
788 11285. https://doi.org/10.1021/jf404046v
789 Rizwan, M., Ali, S., Ali, B., Adrees, M., Arshad, M., Hussain, A., et al., 2019. Zinc and iron oxide
790 nanoparticles improved the plant growth and reduced the oxidative stress and cadmium concentration in
791 wheat. Chemosphere 214, 269-277. https://doi.org/10.1016/j.chemosphere.2018.09.120

792 Rodríguez-Seijo, A., Vega, F.A., Arenas-Lago, D., 2020. Assessment of iron-based and calcium-phosphate
793 nanomaterials for immobilisation of potentially toxic elements in soils from a shooting range berm. J.
794 Environ. Manage. 267, 110640 https://doi.org/10.1016/j.jenvman.2020.110640
795 Ruttkay-Nedecky, B., Krystofova, O., Nejdl, L., Adam V., 2017. Nanoparticles based on essential metals
796 and their phytotoxicity. J. Nanobiotechnology 15, 33. https://doi.org/10.1186/s12951-017-0268-3
797 Seneviratne, M., Rajakaruna, N., Rizwan, M., Madawala, H.M.S.P., Ok, Y.S., Vithanage, M., 2017. Heavy
798 metal-induced oxidative stress on seed germination and seedling development: a critical review. Environ.
799 Geochem. Health. 41, 1813–1831. https://doi.org/10.1007/s10653-017-0005-8
800 Shahid, M., Pourrut, B., Dumat, C., Nadeem, M., Aslam, M., Pinelli, E., 2014. Heavy-metal-induced
801 reactive oxygen species: phytotoxicity and physicochemical changes in plants. In: Whitacre D.M. (Eds).
802 Reviews of Environmental Contamination and Toxicology Volume *232*. Springer, Cham. pp. 1-44.
803 https://doi.org/10.1007/978-3-319-06746-9_1
804 Sharma, A., Sidhu, G., Araniti, F., Bali, A. S., Shahzad, B., Tripathi, D. K., Brestic, M., Skalicky, M.,
805 Landi, M., 2020a. The Role of Salicylic Acid in Plants Exposed to Heavy Metals. Molecules 25(3), 540.
806 https://doi.org/10.3390/molecules25030540
807 Sharma, A., Kapoor, D., Wang, J., Shahzad, B., Kumar, V., Bali, A. S., Jasrotia, S., Zheng, B., Yuan, H.,
808 Yan, D., 2020b. Chromium Bioaccumulation and Its Impacts on Plants: An Overview. Plants 9(1), 100.
809 https://doi.org/10.3390/plants9010100
810 Singh, S., Parihar, P., Singh, R., Singh, V.P., Prasad, S.M., 2016 Heavy Metal Tolerance in Plants: Role of
811 Transcriptomics, Proteomics, Metabolomics, and Ionomics. Front. Plant Sci. 6, 1143.
812 https://doi.org/10.3389/fpls.2015.01143
813 Soares, C., Branco-Neves, S., de Sousa, A., Pereira, R., Fidalgo, F., 2016. Ecotoxicological relevance of
814 nano-NiO and acetaminophen to *Hordeum vulgare* L.: Combining standardized procedures and
815 physiological endpoints. Chemosphere 165, 442-452. https://doi.org/10.1016/j.chemosphere.2016.09.053
816 Soares, C., Branco-Neves, S., de Sousa, A., Azenha, M., Cunha, A., Pereira, R., et al., 2018a. SiO_2
817 nanomaterial as a tool to improve *Hordeum vulgare* L. tolerance to nano-NiO stress. Sci. Total Environ.
818 622-623, 517-525 https://doi.org/10.1016/j.scitotenv.2017.12.002
819 Soares C., Pereira R., Fidalgo F., 2018b. Metal-Based Nanomaterials and Oxidative Stress in Plants:
820 Current Aspects and Overview. In: Faisal, M., Saquib, Q., Alatar, A., Al-Khedhairy, A. (Eds.).

Phytotoxicity of Nanoparticles. Springer, Cham, pp. 197-227. https://doi.org/10.1007/978-3-319-76708-6_8

Soares, C., Carvalho, M.E.A., Azevedo, R.A., Fidalgo, F., 2019a. Plants facing oxidative challenges—A little help from the antioxidant networks. Environ. Exp. Bot. 161, 4-25 https://doi.org/10.1016/j.envexpbot.2018.12.009

Soares, C., Pereira, R., Spormann, S., Fidalgo, F., 2019b. Is soil contamination by a glyphosate commercial formulation truly harmless to non-target plants? – Evaluation of oxidative damage and antioxidant responses in tomato. Environ. Pollut. 247, 256-265 https://doi.org/10.1016/j.envpol.2019.01.063

Soil Science Division Staff., 2017. Soil survey manual. Ditzler, C.; Scheffe, K., Monger H.C.; (Eds.). USDA Handbook 18. Government Printing Office, Washington, D.C.

Song, B., Xu, P., Chen, M., Tang, W., Zeng, G., Gong, J., Zhang, P., et al., 2019. Using nanomaterials to facilitate the phytoremediation of contaminated soil. Crit. Rev. Environ. Sci. Technol. 49, 791-824. https://doi.org/10.1080/10643389.2018.1558891

Soriano-Disla, J.M., Gómez, I., Navarro-Pedreño, J., Jordán, M.M., 2014. The transfer of heavy metals to barley plants from soils amended with sewage sludge with different heavy metal burdens. J. Soils Sediments 14, 687–696. https://doi.org/10.1007/s11368-013-0773-4

Sousa, B., Soares, C., Oliveira, F., Martins, M., Branco-Neves, S., Barbosa, B., et al., 2020. Foliar application of 24-epibrassinolide improves *Solanum nigrum* L. tolerance to high levels of Zn without affecting its remediation potential. Chemosphere 244, 125579. https://doi.org/10.1016/j.chemosphere.2019.125579

Sun, B., Pan, X., Zhou, F., 2012. Species Sensitivity Distribution for Arsenic Toxicity on Plant Based on Soil Culture Data: Implications for Benchmarks of Soil Risk Assessments. In: Zhu, E., Sambath, S., (Eds.) Information Technology and Agricultural Engineering. Advances in Intelligent and Soft Computing, vol 134. Springer, Berlin, Heidelberg. https://doi.org/10.1007/978-3-642-27537-1_103

Tombuloglu, H., Slimani, Y., Tombuloglu, G., Almessiere, M., Baykal, A., 2017. Uptake and translocation of magnetite (Fe_3O_4) nanoparticles and its impact on photosynthetic genes in barley (*Hordeum vulgare* L.). Chemosphere 226, 110-122 https://doi.org/10.1016/j.chemosphere.2019.03.075

Trakal, L., Martínez-Fernández, D., Vítková, M., Komárek, M., 2015. Phytoextraction of metals: modeling root metal uptake and associated processes. In: Ansari, A., Gill, S., Gill, R., Lanza, G., Newman, L. (Eds) Phytoremediation. Springer, Cham. pp. 69-83. https://doi.org/10.1007/978-3-319-10395-2_6

Tripathi, D.K., Shweta, Singh, S., Singh, S., Pandey, R., Singh, V.P., et al., 2017. An overview on manufactured nanoparticles in plants: Uptake, translocation, accumulation and phytotoxicity Plant. Physiol Biochem. 110, 2-12 https://doi.org/10.1016/j.plaphy.2016.07.030

USEPA, 2007. Method 3051A (SW-846): Microwave Assisted Acid Digestion of Sediments, Sludges, and Oils. Revision 1. Washington, DC.

Wan, X., Lei, M., Chen, T., 2020. Review on remediation technologies for arsenic-contaminated soil. Front. Environ Sci. Eng. 14, 24. https://doi.org/10.1007/s11783-019-1203-7

Wang, J.J., Raman, H., Zhang, G.P., Mendham, N., Zhou, M.X. 2006. Aluminium tolerance in barley (*Hordeum vulgare* L.): physiological mechanisms, genetics and screening methods. J. Zhejiang Univ. Sci. B., 7(10), 769-787. https://doi.org/10.1631/jzus.2006.B0769

Wuana, R.A., Okieimen, F.E., 2011. Heavy Metals in Contaminated Soils: A Review of Sources, Chemistry, Risks and Best Available Strategies for Remediation. ISRN Ecol. 2011, 402647. https://doi.org/10.5402/2011/402647

Zdruli, P., Jones, R.J.A., Montanarella, L., 2004. Organic Matter in the Soils of Southern Europe. European Soil Bureau Technical Report, EUR 21083 EN, 16pp. Office for Official Publications of the European Communities, Luxembourg.

Zuverza-Mena, N., Martínez-Fernández, D., Du, W., Hernandez-Viezcas, J.A., Bonilla-Bird, N., López-Moreno, M. L., et al., 2017. Exposure of engineered nanomaterials to plants: Insights into the physiological and biochemical responses-A review. Plant Physiol. Biochem. 110, 236-264. https://doi.org/10.1016/j.plaphy.2016.05.037

871 **Figure captions**

872 **Figure 1**. Root length (a) and root (b) and leaves (c) biomass of *H. vulgare* L. plants in different soils
873 (OECD, S1 and S2), amended (bars with pattern) and non-amended (bars without pattern) with 1% (w/w)
874 nano-Fe_2O_3. Data presented are mean ± SD ($n \geq 3$). Different letters above bars indicate significant
875 differences between soils (OECD, S1 and S2) at $p \leq 0.05$; * above bars denote significant differences
876 between non- and amended soils at $p \leq 0.05$. *The results of two- and one-way ANOVA are shown in*
877 *supplementary material (Tables S3 and S4).*

878 **Figure 2**. Total chlorophylls (a) and carotenoids (b) in leaves of *H. vulgare* L. plants grown in different
879 soils (OECD, S1 and S2), amended (bars with pattern) and non-amended (bars without pattern) with 1%
880 (w/w) nano-Fe_2O_3. Data presented are as mean ± SD ($n \geq 3$). Different letters above bars indicate significant
881 differences between soils (OECD, S1 and S2) at $p \leq 0.05$; * above bars denote significant differences
882 between non-amended and amended soils at $p \leq 0.05$. *The results of two- and one-way ANOVA are shown*
883 *in supplementary material (Tables S3 and S4).*

884 **Figure 3**. $O_2^{\cdot-}$ (a), H_2O_2 (b) and MDA (c) levels in leaves of *H. vulgare* L. plants grown in different soils
885 (OECD, S1 and S2), amended (bars with pattern) and non-amended (bars without pattern) with 1% (w/w)
886 nano-Fe_2O_3. Data presented are as mean ± SD ($n \geq 3$). Different letters above bars indicate significant
887 differences between soils (OECD, S1 and S2) at $p \leq 0.05$; * above bars denote significant differences
888 between non- and amended soils at $p \leq 0.05$. *The results of two- and one-way ANOVA are shown in*
889 *supplementary material (Tables S3 and S4).*

890 **Figure 4**. Proline (a), GSH (b), total ascorbate (c) and relative AsA and DHA (d) levels in leaves of *H.*
891 *vulgare* L. plants grown in different soils (OECD, S1 and S2), amended (bars with pattern) and non-
892 amended (bars without pattern) with 1% (w/w) nano-Fe_2O_3. Data presented are as mean ± SD ($n \geq 3$).
893 Different letters above bars indicate significant differences between soils (OECD, S1 and S2) at $p \leq 0.05$;
894 * above bars denote significant differences between non- and amended soils at $p \leq 0.05$. *The results of two-*
895 *and one-way ANOVA are shown in supplementary material (Tables S3 and S4).*

896 **Figure 5**. SOD (a), CAT (b) and APX (c) activity levels in leaves of *H. vulgare* L. plants grown in different
897 soils (OECD, S1 and S2), amended (bars with pattern) and non-amended (bars without pattern) with 1%
898 (w/w) nano-Fe_2O_3. Data presented are as mean ± SD ($n \geq 3$). Different letters above bars indicate significant

899 differences between soils (OECD, S1 and S2) at $p \leq 0.05$; * above bars denote significant differences
900 between non- and amended soils at $p \leq 0.05$. *The results of two- and one-way ANOVA are shown in*
901 *supplementary material (Tables S3 and S4).*

Table 1. Physical and chemical properties of the OECD, S1 and S2 soil samples prepared in the laboratory and collected nearby the Estarreja Chemical Complex (ECC), Portugal.

Soil properties	**Units**	**OECD soil**	**S1**	**S2**
Physicochemical properties				
pH $_{H2O}$		6.09 ± 0.23	4.69 ± 0.05	6.22 ± 0.07
Electrical conductivity	mS/m	-	0.4 ± 0.12	0.22 ± 0.09
Organic matter	%	4.48 ± 0.34	2.54 ± 0.42	5.73 ± 0.78
Water Holding Capacity	%	29.2 ± 4.1	34.3 ± 0.8	40.2 ± 2.0
Soil texture		Sandy loam	Sandy loam	Loamy fine sand
Sand	%	77.2 ± 1.5	75.9 ± 1.2	87.3 ± 1.5
Silt	%	15.3 ± 2.1	16.6± 1.3	3.50 ± 1.17
Clay	%	7.53 ± 0.81	7.45 ± 0.70	7.97 ± 0.45
Pseudo total contents (mg kg^{-1})				
Element	**S1**	**S2**	**PT-RV**	**CDN-SQG**
Al	6788 ± 1063	8150 ± 208	-	-
As	**59.8 ± 13.3**	**1344 ± 75**	11	12
Ba	19.4 ± 3.0	286 ± 5	390	750
Cd	0.14 ± 0.07	0.91 ± 0.10	1	1.4
Cr	6.26 ± 1.37	12.1 ± 0.3	160	64
Cu	14.6 ± 2.6	**202 ± 2**	140	63
Fe	4316 ± 992	8366 ± 86	-	-
K	920 ± 121	1269 ± 17	-	-
Mg	1142 ± 92	1083 ± 39	-	-
Mn	46.9 ± 18.4	43.2 ± 0.6	-	-
Ni	4.57 ± 0.93	8.41 ± 0.14	100	45
P	278 ± 116	653 ± 39	-	-
Pb	22.6 ± 2.9	**490 ± 22**	46	70
Sb	< 0.02	6.14 ± 0.09	7.5	20
Zn	58.2 ± 5.8	**309 ± 7**	340	250

Data presented are mean ± SD (standard deviation) ($n \geq 3$) for physicochemical parameters.

PT-RV Reference values for soils < 2m deep (agricultural), recommended by the Portuguese Environmental Agency (APA 2019); CDN-SQG Canadian Soil Quality Guidelines according to the agricultural land use (CCME 2007, 2018). Bold numbers highlight values that are above the Portuguese and/or the Canadian guidelines for agricultural soils.

Table 2. Available contents of analyzed elements from studied soils: Non-amended and amended with nano-Fe_2O_3 and corresponding extraction efficiencies (EE%).

Element	**$CaCl_2$-extractable (mg kg^{-1})**							
	S1				**S2**			
	Non-amended	**EE (%)**	**nano-Fe_2O_3**	**EE (%)**	**Non-amended**	**EE (%)**	**nano-Fe_2O_3**	**EF (%)**
Al	4.85 ± 0.16	0.07	2.42 ± 0.07*	0.04*	2.27 ± 0.19	0.03	1.99 ± 0.32	0.02
As	0.06 ± 0.01	0.10	*b.d.l.*	-	4.11 ± 0.41	0.31	5.37 ± 0.44	0.40
Ba	0.38 ± 0.01	1.94	0.41 ± 0.01	2.11	6.48 ± 0.65	2.27	12.1 ± 0.1*	4.24*
Cd	0.03 ± 0.01	23.1	0.03 ± 0.01	24.0	0.03 ± 0.01	3.60	0.02 ± 0.01	2.41
Cr	*b.d.l.*	-	*b.d.l.*	-	*b.d.l.*	-	*b.d.l.*	-
Cu	*b.d.l.*	-	*b.d.l.*	-	0.32 ± 0.03	0.16	0.45 ± 0.04	0.22
Fe	0.40 ± 0.24	0.01	0.44 ± 0.01	0.02	4.50 ±0.40	0.05	3.68 ± 0.55	0.03
K	5.3 ± 2.6	0.58	10.1 ± 1.4*	1.09	88.5 ± 8.7	6.98	68.0 ± 2.1*	5.36
Mg	21.0 ± 0.7	1.84	83.1 ± 2.7*	7.28*	51.4 ± 5.2	4.75	57.8 ± 3.8	5.34
Mn	0.80 ± 0.02	1.71	12.2 ± 0.3*	26.0*	0.33 ± 0.04	0.77	6.37 ± 0.05*	14.8*
Ni	0.10 ± 0.02	2.21	0.08 ± 0.01	1.72	0.23 ± 0.02	2.72	0.04 ± 0.01*	0.42*
P	*b.d.l.*	-	*b.d.l.*	-	0.98 ± 0.12	0.15	1.75 ± 0.43	0.27
Pb	0.03 ± 0.02	0.14	*b.d.l.*	-	0.45 ± 0.04	0.09	0.25 ± 0.20	0.05
Sb	*b.d.l.*	-	*b.d.l.*	-	0.06 ± 0.01	0.99	0.09 ± 0.01*	1.52*
Zn	3.52 ± 0.04	6.06	1.72 ± 0.04*	2.96*	5.73 ± 0.58	1.85	2.16 ± 0.05*	0.70*
Element	**EDTA-extractable (mg kg^{-1})**							
	S1				**S2**			
	Non-amended	**EE (%)**	**nano-Fe_2O_3**	**EE(%)**	**Non-amended**	**EE (%)**	**nano-Fe_2O_3**	**EE (%)**
Al	172 ± 5	2.54	157 ± 28	2.31*	217 ± 17	2.66	185 ± 28	2.22
As	9.56 ± 0.08	16.0	7.3 ± 1.2*	12.3	141 ± 16	10.5	124 ± 20.0	9.21
Ba	1.57 ± 0.05	8.11	1.67 ± 0.20	8.63	60.5 ± 4.4	21.2	64.1 ± 8.2	22.4
Cd	0.06 ± 0.01	44.7	0.05 ± 0.01	36.1	0.43 ± 0.03	47.3	0.30 ± 0.03*	33.1*
Cr	0.15 ± 0.03	2.46	0.24 ± 0.03	3.86	0.32 ± 0.02	2.66	0.30 ± 0.02	1.66
Cu	3.47 ± 0.09	23.8	3.55 ± 0.55	24.3	99.7 ± 7.1	49.3	59.1 ± 6.3*	29.2*
Fe	455 ± 9	10.6	463 ± 76	10.7	544 ± 55	6.50	510 ± 72	6.10
K	*b.d.l.*	-	*b.d.l.*	-	101 ± 6	7.93	31.2 ± 3.4*	2.46*
Mg	20.0 ± 1.3	1.75	38.8 ± 8.2*	3.40	118 ± 12	10.9	72.4 ± 7.4*	6.68
Mn	4.72 ± 0.10	10.1	9.7 ± 1.4*	20.6*	11.2 ± 1.2	25.9	18.0 ± 1.8*	41.7*
Ni	0.31 ± 0.03	6.69	0.25 ± 0.04	5.51	0.66 ± 0.05	7.91	0.41 ± 0.01*	3.21*
P	58.9 ± 1.1	21.2	51.0 ± 7.2	18.3	91.4 ± 5.7	14.0	79.4 ± 9.3	12.2
Pb	9.72 ± 0.39	43.0	8.3 ± 1.1	36.8	206 ± 29	41.9	132 ± 17*	27.0*
Sb	*b.d.l.*	-	*b.d.l.*	-	0.59 ± 0.06	9.64	0.43 ± 0.06*	7.01*
Zn	7.93 ± 0.55	13.6	4.22 ± 0.79*	7.26	90.2 ± 6.5	23.2	52.6 ± 5.3*	17.0*

Data presented are mean ± SD ($n \geq 3$); *b.d.l.* Below detection limit,. * denote significant differences between non- and amended soils at $p \leq 0.05$.

Table 3. Contents and bioconcentration factor (BCF) of analyzed elements in leaves of barley plants exposed to studied soils (OECD soil as control, S1 and S2): non-amended and amended with nano-Fe_2O_3.

Element	Units	OECD soil		S1		S2	
		Non-amended	nano-Fe_2O_3	Non-amended	nano-Fe_2O_3	Non-amended	nano-Fe_2O_3
		Leaves contents					
Al	mg kg^{-1}	40 ± 17	35 ± 10	41.7 ± 5.1	39 ± 12	34 ± 14	30 ± 15
As	mg kg^{-1}	0.81 ± 0.15	0.35 ± 0.16*	5.2 ± 1.3	5.4 ± 1.4	20 ± 14	22 ± 9
Ba	mg kg^{-1}	4.64 ± 0.93	4.4 ± 1.4	5.3 ± 1.15	5.51 ± 0.74	27.5 ± 9.2	30.9 ± 4.4
Cd	mg kg^{-1}	*b.d.l.*	*b.d.l.*	0.26 ± 0.02	0.20 ± 0.03*	0.14 ± 0.06	0.14 ± 0.03
Cr	mg kg^{-1}	0.58 ± 0.13	0.62 ± 0.29	0.77 ± 0.18	1.36 ± 0.95	3.44 ± 1.97	1.79 ± 0.88
Cu	mg kg^{-1}	5.71 ± 0.79	6.3 ± 2.0	7.11 ± 0.34	7.9 ± 1.0	6.4 ± 2.3	8.6 ± 1.4
Fe	mg kg^{-1}	59 ± 16	102 ± 9*	122 ± 29	95 ± 10	74 ± 8	90 ± 28
K	g kg^{-1}	59.4 ± 7.1	52.6 ± 5.5	53.2 ± 5.5	48.4 ± 3.1	47 ± 10	54 ± 13
Mg	g kg^{-1}	2.06 ± 0.36	2.03 ± 0.54	1.89 ± 0.58	1.90 ± 0.66	1.52 ± 0.29	1.62 ± 0.26
Mn	mg kg^{-1}	51 ± 12	40 ± 24	74.7 ± 5.6	70.7 ± 7.1	15.5 ± 2.6	17.9 ± 2.3
Ni	mg kg^{-1}	0.14 ± 0.04	0.17 ± 0.10	0.32 ± 0.07	0.25 ± 0.03	0.23 ± 0.01	0.16 ± 0.06
P	g kg^{-1}	5.0 ± 1.0	4.2 ± 1.4	4.2 ± 1.1	3.58 ± 0.76	4.2 ± 1.9	2.60 ± 0.54
Pb	mg kg^{-1}	0.40 ± 0.20	0.40 ± 0.12	0.51 ± 0.35	0.25 ± 0.10	1.4 ± 1.0	1.08 ± 0.42
Sb	mg kg^{-1}	0.06 ± 0.06	0.02 ± 0.01	0.04 ± 0.01	0.05 ± 0.01	0.22 ± 0.01	0.03 ± 0.01*
Zn	mg kg^{-1}	48.2 ± 6.8	48 ± 12	67.2 ± 4.2	47.7 ± 5.8*	50.2 ± 14	59 ± 12
Element		**Bioconcentration factor (BCF)**					
Al		n.d.	n.d.	0.01 ± 0.01	0.01 ± 0.01	0.01 ± 0.00	0.01 ± 0.00
As		n.d.	n.d.	0.09 ± 0.02	0.09 ± 0.02	0.01 ± 0.01	0.02 ± 0.01
Ba		n.d.	n.d.	0.27 ± 0.06	0.28 ± 0.04	0.10 ± 0.03	0.11 ± 0.02
Cd		n.d.	n.d.	1.53 ± 0.30	1.17 ± 0.39	0.16 ± 0.07	0.15 ± 0.03
Cr		n.d.	n.d.	0.12 ± 0.03	0.16 ± 0.16	0.28 ± 0.16	0.15 ± 0.07
Cu		n.d.	n.d.	0.49 ± 0.02	0.54 ± 0.07	0.03 ± 0.01	0.04 ± 0.01
Fe		n.d.	n.d.	0.03 ± 0.01	0.02 ± 0.00	0.01 ± 0.00	0.01 ± 0.00
Mn		n.d.	n.d.	1.59 ± 0.12	1.51 ± 0.15	0.36 ± 0.06	0.31 ± 0.21
Ni		n.d.	n.d.	0.07 ± 0.02	0.06 ± 0.01	0.03 ± 0.00	0.01 ± 0.01*
Pb		n.d.	n.d.	0.02 ± 0.02	0.01 ± 0.00	0.01 ± 0.00	0.01 ± 0.00
Sb		n.d.	n.d.	n.d.	n.d.	0.04 ± 0.00	0.01 ± 0.00*
Zn		n.d.	n.d.	1.16 ± 0.07	0.82 ± 0.10*	0.16 ± 0.04	0.19 ± 0.04

Data presented are mean ± SD. *n.d.* Not determined. *b.d.l.* Below detection limit. * denote significant differences between non- and amended soils for each element at $p \leq 0.05$. *The results of two-way ANOVA are shown in the supplementary material (Tables S1 and S2).*

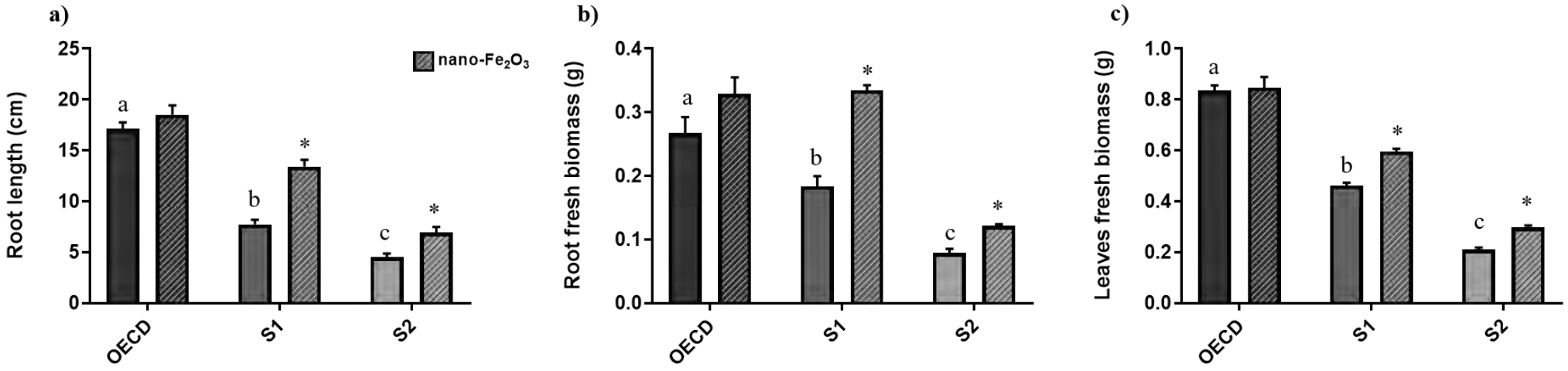
a)
Root length (cm)
nano-Fe2O3
25
20
15
10
5
0
a
b
c
*
*
OECD
S1
S2
b)
Root fresh biomass (g)
0.4
0.3
0.2
0.1
0.0
a
b
c
*
*
OECD
S1
S2
c)
Leaves fresh biomass (g)
1.0
0.8
0.6
0.4
0.2
0.0
a
b
c
*
*
OECD
S1
S2

Figure 1.

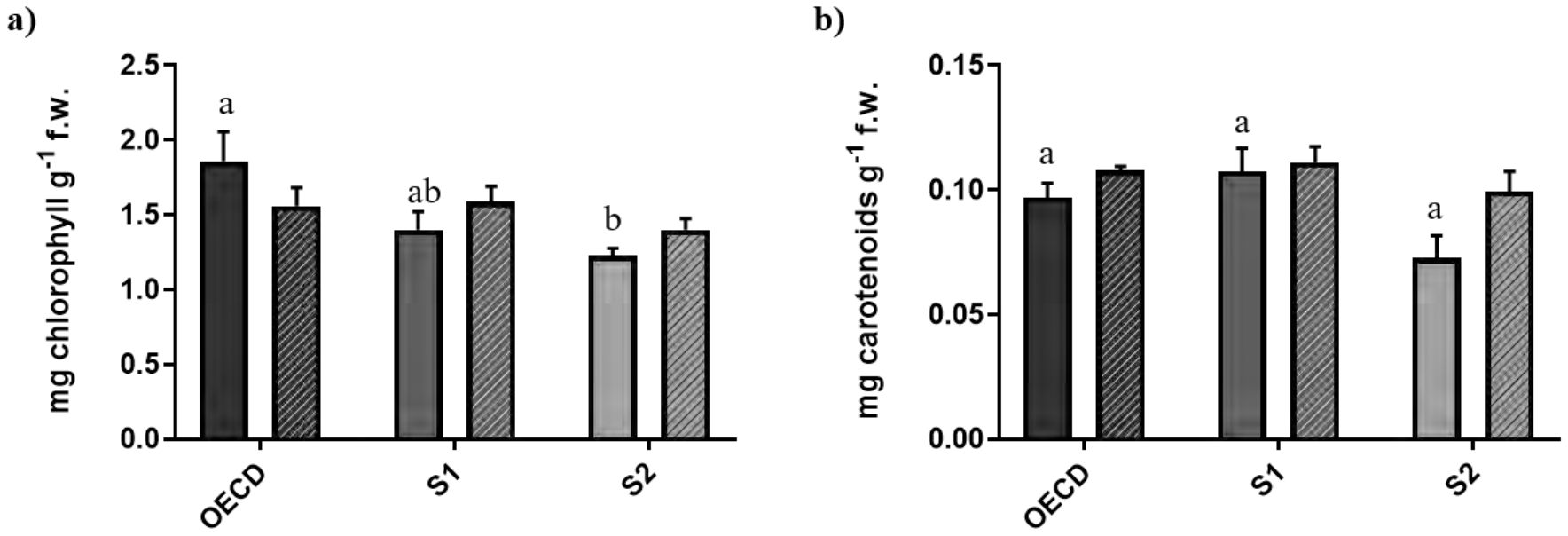
a)
mg chlorophyll g-1 f.w.
2.5
2.0
1.5
1.0
0.5
0.0
a
ab
b
OECD
S1
S2
b)
mg carotenoids g-1 f.w.
0.15
0.10
0.05
0.00
a
a
a
OECD
S1
S2

Figure 2.

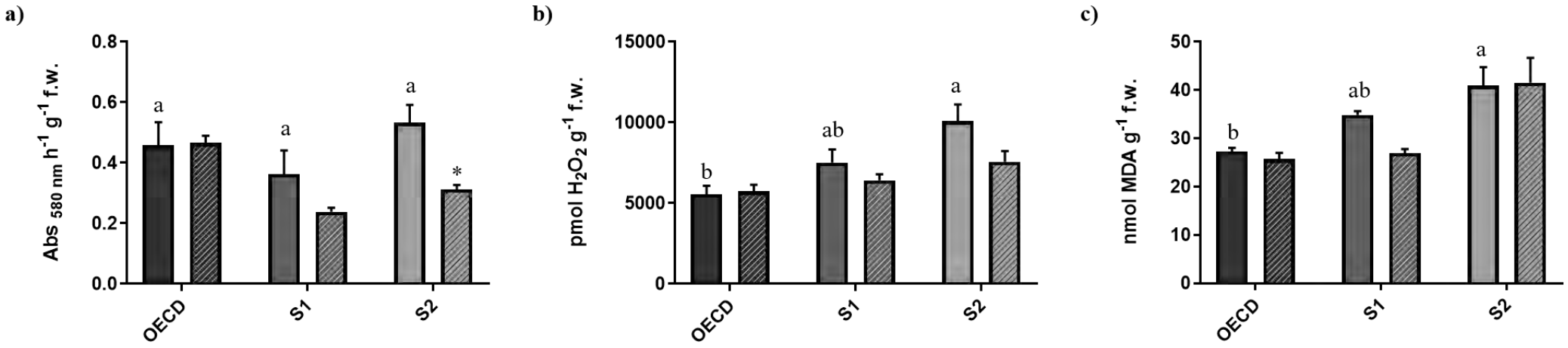
a)
Abs 580 nm h-1 g-1 f.w.
0.8
0.6
0.4
0.2
0.0
a
a
a
*
OECD
S1
S2
b)
pmol H2O2 g-1 f.w.
15000
10000
5000
0
b
ab
a
OECD
S1
S2
c)
nmol MDA g-1 f.w.
50
40
30
20
10
0
b
ab
a
OECD
S1
S2

Figure 3.

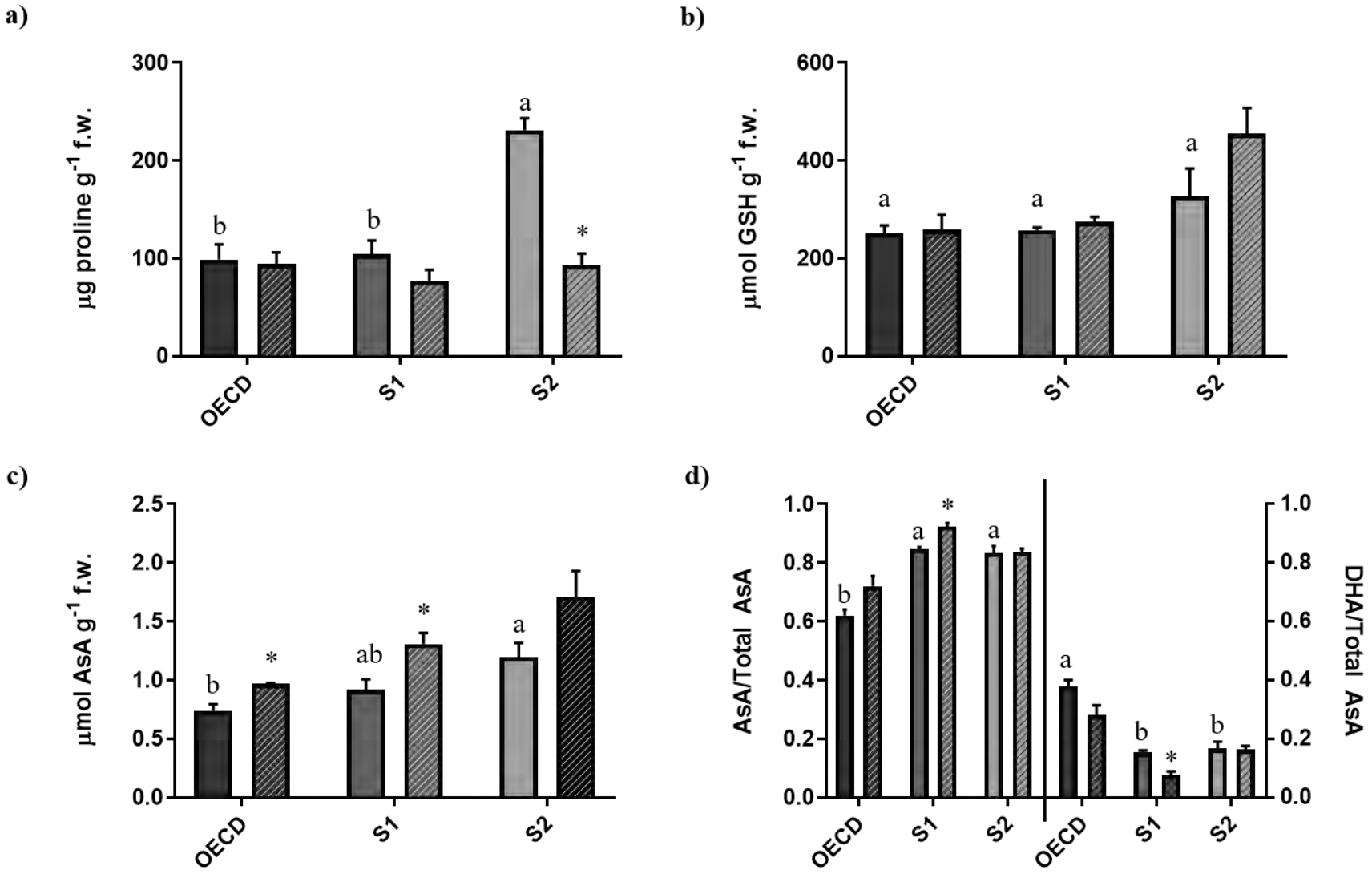
a)
b)
c)
d)
µg proline g-1 f.w.
µmol GSH g-1 f.w.
µmol AsA g-1 f.w.
AsA/Total AsA
DHA/Total AsA
OECD
S1
S2

Figure 4.

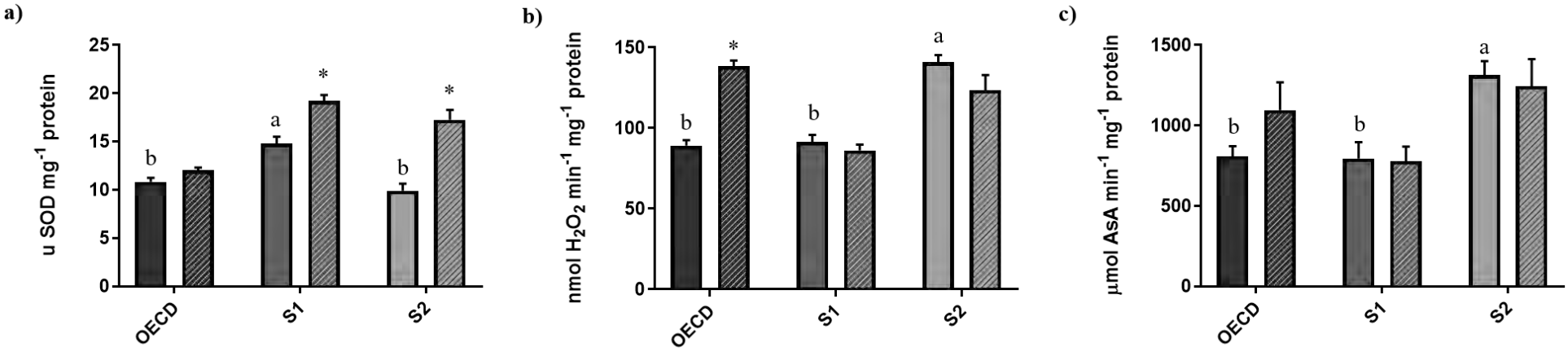
a)
u SOD mg-1 protein
25
20
15
10
5
0
b
a
b
*
*
OECD
S1
S2
b)
nmol H2O2 min-1 mg-1 protein
150
100
50
0
b
b
a
*
OECD
S1
S2
c)
µmol AsA min-1 mg-1 protein
1500
1000
500
0
b
b
a
OECD
S1
S2

Figure 5.

SUPPLEMENTARY MATERIAL

Nano-Fe_2O_3 as a tool to restore plant growth in contaminated soils - assessment of potentially toxic elements (bio)availability and redox homeostasis in *Hordeum vulgare* L.

Andrés Rodríguez-Seijo[1,2*], Cristiano Soares[2,3*], Sónia Ribeiro[2,3], Berta Ferreiro Amil[3,4], Carla Patinha[5], Anabela Cachada[1,2], Fernanda Fidalgo[2,3], Ruth Pereira[2,3]

[1]CIIMAR - Interdisciplinary Centre of Marine and Environmental Research (CIIMAR), University of Porto, Terminal de Cruzeiros do Porto de Leixões, Av. General Norton de Matos s/n, 4450-208, Matosinhos, Portugal

[2]Department of Biology, Faculty of Sciences of University of Porto (FCUP), 4169-007 Porto, Portugal

[3]GreenUPorto—Sustainable Agrifood Production Research Centre and INOV4AGRO, Rua do Campo Alegre s/n, Faculty of Sciences of University of Porto (FCUP), 4169-007 Porto, Portugal

[4]Faculdade de Bioloxía, Universidade de Santiago de Compostela, Santiago de Compostela, Spain

[5]Department of Geosciences & GEOBIOTEC, University of Aveiro, Campus de Santiago, Aveiro, 3810-193, Portugal

* These authors contributed equally to this work and, therefore, should be both considered as first co-authors

‡*Corresponding author:*

Andrés Rodríguez-Seijo (andres.seijo@fc.up.pt)

List of items

Figures: 1

Tables: 4

Figure S1. Location of the Estarreja Chemical Complex and of the sampling sites

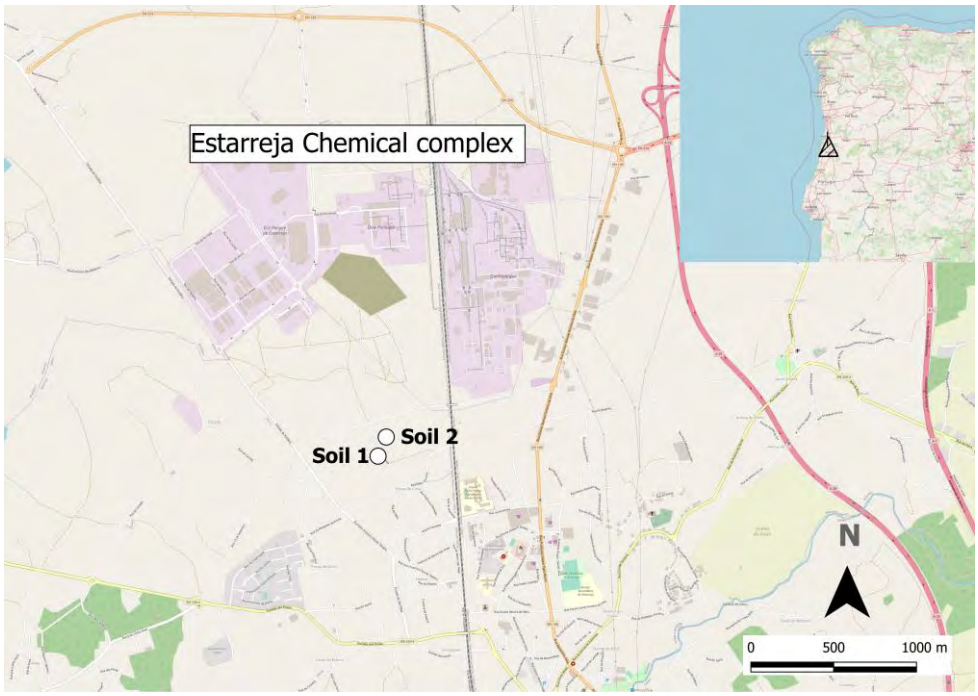

Table S1. Summary of two-way ANOVA statistical data with type of substrate and application of nano-Fe_2O_3 defined as fixed factors for PTEs contents in leaves. Significant effects are highlighted at bold.

Element	Factors		Interaction
	Type of substrate	***Application of nano-Fe_2O_3***	
Al	F (2, 17) = 0.829 ; p = 0.4531	F (1, 17) = 0.424 ; p = 0.5235	F (2, 17) = 0.015 ; p = 0.9850
As	**F (2, 20) = 22.91 ; p < 0.0001**	F (1, 20) = 0.04545 ; p = 0.833	F (2, 20) = 0.0734 ; p = 0.9295
Ba	**F (2, 19) = 92.36 ; p < 0.0001**	F (1, 19) = 0.4364 ; p = 0.5168	F (2, 19) = 0.4633 ; p = 0.6362
Cd	**F (2, 20) = 132.3 ; p < 0.0001**	**F (1,20) = 4.427 ; p = 0.0482**	F (2, 20) = 3.175 ; p = 0.0634
Cr	**F (2, 15) = 9.619 ; p = 0.0021**	F (1, 15) = 0.774 ; p = 0.3918	F (2, 15) = 2.828 ; p = 0.0908
Cu	F (2, 18) = 2.755 ; p = 0.0904	F (1, 18) = 3.811 ; p = 0.0667	F (2, 18) = 0.6195 ; p =0.5493
Fe	**F (2, 21) = 4.210 ; p = 0.0290**	F (1, 21) = 1.440 ; p = 0.2428	**F (2, 21) = 5.003 ; p = 0.0167**
K	F (2, 18) = 1.126 ; p = 0.346	F (1, 18) = 0.2065 ; p = 0.6550	F (2, 18) = 1.770 ; p = 0.1987
Mg	F (2, 23) = 2.378 ; p = 0.1152	F (1, 23) = 0.029 ; p = 0.8655	F (2, 23) = 0.0498 ; p = 0.951
Mn	**F (2, 16) = 26.8 ; p < 0.0001**	F (1, 16) = 0.5192 ; p = 0.4816	F (2, 16) = 0.4502 ; p =0.6453
Ni	**F (2, 14) = 7.24 ; p = 0.0069**	F (1, 14) = 1.235 ; p = 0.283	F (2, 14) = 1.281 ; p = 0.3084
P	F (2, 19) = 2.25 ; p = 0.1318	F (1, 19) = 4.298 ; p = 0.0520	F (2, 19) = 0.4215 ; p = 0.6614
Pb	**F (2, 17) = 9.262 ; p = 0.0019**	F (1, 17) = 1.139 ; p = 0.3008	F (2, 17) = 0.30 ; p = 0.7381
Sb	**F (2, 13) = 16.39 ; p = 0.0003**	**F (1, 13) = 31.04 ; p < 0.0001**	**F (2, 13) = 20.11 ; p = 0.0001**
Zn	F (2, 16) = 2.116 ; p = 0.1530	F (1, 16) = 0.8497 ; p = 0.3703	**F (2, 16) = 4.306 ; p = 0.0319**

Table S2. Summary of one-way ANOVA statistical data performed for each factor (type of substrate and application of nano-Fe_2O_3) and for leaves contents. Significant effects are highlighted at bold. Empty spaces represent cases where 2-way ANOVA did not reveal significant differences for each factor. In cases where a significant interaction was found, the F value was adjusted to analyze the simple main effects of each fixed factor.

		Application of nano-Fe_2O_3		
Element	***Type of substrate***	***OECD***	**S1**	**S2**
Al	F (2,8) = 0.3314; p = 0.7273	F (1,6) = 0.223; p = 0.653	F (1,5) = 0.101; p = 0.763	F (1,6) = 0.130; p = 0.731
As	**F (2,9) = 6.56 ; p = 0.017**	**F (1,6) = 16.975 ; p = 0.006**	F (1,7) = 0.054 ; p = 0.822	F (1,7) = 0.66 ; p = 0.804
Ba	**F (2,9) = 23.56 ; p < 0.0001**	F (1,6) = 0.092 ; p = 0.771	F (1,6) = 0.136 ; p = 0.725	F (1,7) = 0.544 ; p = 0.485
Cd	**F (2,9) = 58.92 ; p < 0.0001**	-	**F (1,6) = 17.22 ; p = 0.006**	F (1,6) = 0.045 ; p = 0.839
Cr	**F (2,9) = 8.546 ; p = 0.010**	F (1,6) = 0.050 ; p = 0.830	F (1,6) = 1.612; p = 0.260	F (1,4) = 1.757 ; p = 0.256
Cu	F (2,9) = 0.967 ; p = 0.416	F (1,6) = 0.318 ; p = 0.593	F (1,6) = 2.326 ; p = 0.178	F (1,6) = 2.431 ; p = 0.170
Fe	F (2,9) = 7.63 ; p = 0.0083	**F (1,6) = 21.573 ; p = 0.04**	F (1,7) = 3.014 ; p = 0.126	F (1,8) = 0.778 ; p = 0.404
K	F (2,9) = 2.41 ; p = 0.145	F (1,6) = 2.298 ; p = 0.180	F (1,6) = 2.284 ; p = 0.181	F (1,6) = 0.771 ; p = 0.414
Mg	F (2,9) = 1.74; p = 0.219	F (1,8) = 0.012 ; p = 0.916	F (1,8) = 0.002 ; p = 0.967	F (1,7) = 0.334 ; p = 0.582
Mn	**F (2,7) = 37.442 ; p < 0.0001**	F (1,6) = 0.08 ; p = 0.787	F (1,5) = 0.636 ; p = 0.461	F (1,4) = 1.420 ; p = 0.299
Ni	**F (2,9) = 9.079 ; p = 0.022**	F (1,5) = 0.269 ; p = 0.626	F (1,5) = 2.814; p = 0.154	F (1,4) = 2.151 ; p = 0.216
P	F (2,9) = 0.473 ; p = 0.638	F (1,6) = 0.906 ; p = 0.378	F (1,6) = 0.761; p = 0.416	F (1,7) = 3.008 ; p = 0.126
Pb	F (2,9) = 3.093 ; p = 0.101	F (1,6) = 0.000 ; p = 0.984	F (1,6) = 1.925 ; p = 0.215	F (1,5) = 0.357 ; p = 0.576
Sb	**F (2,9) = 17.775 ; p = 0.002**	F (1,6) = 0.762 ; p = 0.447	F (1,6) = 1.944 ; p = 0.222	**F (1,2) = 330.882 ; p = 0.003**
Zn	**F (2,9) = 5.95 ; p = 0.026**	F (1,6) = 0.01; p = 0.974	**F (1,6) = 29.376 ; p = 0.002**	F (1,4) = 0.692 ; p = 0.452

Table S3. Summary of two-way ANOVA statistical data with type of substrate and application of nano-Fe_2O_3 defined as fixed factors for the biochemical parameters. Significant effects are highlighted at bold.

Parameter	Factors		Interaction
	Type of substrate	***Application of nano-Fe_2O_3***	
Root length	**F (2, 40) = 188.8; *p* < 0.0001**	**F (1, 40) = 39.73; *p* < 0.0001**	**F (2, 40) = 6.622; *p* = 0.0033**
Root biomass	**F (2, 24) = 77.00; *p* < 0.0001**	**F (1, 24) = 38.01; *p* < 0.0001**	**F (2, 24) = 5.837; *p* = 0.0086**
Leaf biomass	**F (2, 26) = 317.9; *p* < 0.0001**	**F (1, 26) = 16.56; *p* = 0.0004**	**F (2, 26) = 3.712; *p* = 0.0382**
Total chlorophylls	**F (2, 14) = 4.941; *p* = 0.0238**	F (1, 14) = 0.04963; *p* = 0.8269	F (2, 14) = 2.560; *p* = 0.1129
Carotenoids	**F (2, 12) = 5.640; *p* = 0.0188**	**F (1, 12) = 5.586; *p* = 0.0358**	F (2, 12) = 1.391; *p* = 0.2862
H_2O_2	**F (2, 15) = 9.426; *p* = 0.0022**	F (1, 15) = 3.520; *p* = 0.0802	F (2, 15) = 1, 698; *p* = 0.2164
$O_2^{\cdot-}$	**F (2, 13) = 4.718; *p* = 0.0288**	**F (1, 13) = 6.604; *p* = 0.0233**	F (2, 13) = 2.306; *p* = 0.1390
Lipid peroxidation	**F (2, 20) = 16.97; *p* < 0.0001**	F (1, 20) = 1.874; *p* = 0.1862	F (2, 20) = 1.323; *p* = 0.2885
Proline	**F (2, 20) = 14.26; *p* = 0.0001**	**F (1, 20) = 22.02; *p* = 0.0001**	**F (2, 20) = 12.47; *p* = 0.0001**
Total ascorbate	**F (2, 13) = 12.88; *p* = 0.0008**	**F (1, 13) = 14.68; *p* = 0.0021**	F (2, 13) = 0.7102; *p* = 0.5096
Relative AsA	**F (2, 12) = 60.49; *p* < 0.0001**	**F (1, 12) = 12.90; *p* = 0.0037**	F (2, 12) = 3.040; *p* = 0.0855
Relative DHA	**F (2, 12) = 60.49; *p* < 0.0001**	**F (1, 12) = 12.90; *p* = 0.0037**	F (2, 12) = 3.040; *p* = 0.0855
GSH	**F (2, 19) = 7.305; *p* = 0.0044**	F (1, 19) = 2.153; *p* = 0.1587	F (2, 19) = 1.424; *p* = 0.2654
SOD	**F (2, 13) = 35.51; *p* < 0.0001**	**F (1, 13) = 60.66; *p* < 0.0001**	**F (2, 13) = 9.828; *p* = 0.0025**
CAT	**F (2, 11) = 33.28; *p* < 0.0001**	F (1, 11) = 3.874; *p* = 0.0748	**F (2, 11) = 19.01; *p* = 0.0003**
APX	**F (2, 11) = 9.975; *p* = 0.0034**	F (1, 11) = 0.5086; *p* = 0.4906	F (2, 11) = 1.267; *p* = 0.3197

Table S4. Summary of one-way ANOVA statistical data performed for each factor (type of substrate and application of nano-Fe_2O_3) the biochemical parameters. Significant effects are highlighted at bold. Empty spaces represent cases where 2-way ANOVA did not reveal significant differences for each factor. In cases where a significant interaction was found, the F value was adjusted to analyze the simple main effects of each fixed factor.

		Application of nano-Fe_2O_3		
Parameter	***Type of substrate***	***OECD***	**S1**	**S2**
Root length	**F_{adj} (2, 19) = 100.242; p < 0.0001**	F_{adj} (1, 11) = 2.154; p = 0.17	**F_{adj} (1, 14) = 45.27; p < 0.0001**	**F_{adj} (1, 15) = 8.799; p < 0.0001**
Root biomass	**F_{adj} (2, 12) = 45.00; p < 0.0001**	**F_{adj} (1, 8) = 9.00; p = 0.017**	**F_{adj} (1, 8) = 57.00; p < 0.0001**	F_{adj} (1, 7) = 5.00; p = 0.06
Leaf biomass	**F_{adj} (2, 13) = 177.67; p < 0.0001**	F_{adj} (1, 9) = 0.00; p = 0.1	**F_{adj} (1, 9) = 16.3; p < 0.029**	**F_{adj} (1, 8) = 5.6; p < 0.045**
Total chlorophylls	**F (2, 7) = 5.392; p = 0.038**	-	-	-
Carotenoids	F (2, 6) = 4.848; p = 0.056	F (1, 4) = 3.334; p = 0.142	F (1, 4) = 0.108; p = 0.759	F (1, 4) = 4.897; p = 0.091
H_2O_2	**F (2, 8) = 6.424; p = 0.022**	-	-	-
$O_2^{\cdot-}$	F (2, 7) = 1.545; p = 0.278	F (1, 4) = 0.008; p = 0.931	F (1, 4) = 2.517; p = 0.188	**F (1, 5) = 9.870; p = 0.026**
Lipid peroxidation	**F (2, 10) = 9.264; p < 0.005**	-	-	-
Proline	**F_{adj} (2, 17) = 49.19; p < 0.0001**	F_{adj} (1, 6) = 0.032; p = 0.860	**F_{adj} (1, 4) = 2.52; p = 0.19**	**F_{adj} (1, 6) = 78.52; p < 0.0001**
Total ascorbate	**F (2, 7) = 5.559; p = 0.036**	**F (1, 4) = 16.514; p = 0.015**	**F (1, 4) = 9.428; p = 0.037**	F (1, 5) = 4.725; p = 0.082
Relative AsA	**F (2, 6) = 47.478; p < 0.0001**	F (1, 4) = 6.122; p = 0.069	**F (1, 4) = 31.118; p = 0.005**	F (1, 4) = 0.016; p = 0.905
Relative DHA	**F (2, 6) = 47.478; p < 0.0001**	F (1, 4) = 6.122; p = 0.069	**F (1, 4) = 31.118; p = 0.005**	F (1, 4) = 0.016; p = 0.905
GSH	F (2, 6) = 4.210; p = 0.072	-	-	-
SOD	**F_{adj} (2, 6) = 14.14; p = 0.005**	F_{adj} (1, 4) = 1.511; p = 0.28	**F_{adj} (1, 5) = 22.92; p = 0.0049**	**F_{adj} (1, 4) = 65.73; p = 0.0013**
CAT	**F_{adj} (2, 6) = 29.95; p = 0.0008**	**F_{adj} (1, 3) = 34.09; p = 0.0043**	**F_{adj} (1, 4) = 0.47; p = 0.530**	F_{adj} (1, 4) = 5.26; p = 0.08
APX	**F (2, 6) = 16.349; p = 0.004**	-	-	-